Characterizing some major Archean faults at depth in the Superior craton, North America

David B. Snyder[1,2], Jack M. Simmons[2], John A. Ayer[1,2], Mostafa Naghizadeh[2], Ademola Q. Adetunji[2],
Taus R. C. Jørgensen[2], Graham J. Hill[3], Eric A. Roots[2], and Saeid Cheraghi[2]

[1] Harquail School of Earth Sciences, Laurentian University, 935 Ramsey Lake Road, Sudbury, ON, Canada, P3E 2C6

[2] Metal Earth, Mineral Exploration Research Centre (MERC), Laurentian University, 935 Ramsey Lake Road, Sudbury, ON, Canada, P3E 2C6

[3] Institute of Geophysics, Czech Academy of Sciences, Prague, Czech Republic

Correspondence to: David B. Snyder (dbsnyder1867@gmail.com)

Abstract. The geometry of ancient faults at depth can only be mapped by high-resolution geophysical surveys such as seismic reflection profiling. Recent deep (35–48 km) reflection profiles acquired across the Archean southern Superior craton of North America provided such data with which to map in 3-D some major shear zones, many of which are associated with significant orogenic gold or volcanogenic massive sulfide (VMS) deposits. Most faults are (re)interpreted as thrusts; a few appear as sub-vertically aligned breaks in prominent reflectors. Sub-vertical faults possibly originated as syn-volcanic transform faults. Thrusting probably relates to the dominant phase of folding and horizontal shortening strain that occurred during the regional crustal deformation, mineralization and peak metamorphism at 2.72–2.66 Ga, associated with the Kenoran orogeny. Most deformation after this orogenic event resulted in modest lateral movement. Coincident magnetotelluric (MT) surveys indicate pervasive conductive minerals such as graphite/carbon and sulfides, exist within the mid-crust and in near-vertical channels within the more brittle and resistive upper (greenstone) crust. Many such channels, but not all, coincide with fault zones and mineral deposits. Palinspastic and paleomagnetic-based reconstructions suggest many faults had multiple periods of activity with changing vertical to horizontal offsets. Some faults appear paired, partitioning normal and oblique strains on vertical shear zones and dipping thrust zones, respectively.

1. 1 Introduction

Major Archean-age faults typically have more cryptic descriptions than do neotectonic faults due to an accumulation of overprinting structures, poor surface exposures, extensive metamorphism, or a lack of supporting syn-tectonic observations such as earthquakes. Conversely, observations of these faults at depth are sometimes enhanced by the stronger propagation of seismic waves within their host crystalline rocks. High-resolution geophysical techniques, including as reflection profiling, have consequently been employed to resolve the geometry of ancient crustal-scale faults, particularly within the

Superior craton of North America (e.g., Calvert et al., 2004; Snyder et al., 2008), where shear zones and faults are spatially
35   associated with world-class gold deposits (e.g., Cadillac-Larder Lake and Porcupine-Destor faults; Poulsen, 2017; Dubé and
Mercier-Langevin, 2020). The crust of the Superior craton (Fig. 1), the world's largest exposure of Archean crust, has
historically been recognized as consisting of three layers, colloquially known as the upper-crustal greenstone layer, the
middle crustal layer, and the lower crustal later (Percival and West, 1994; Benn and Peschler, 2005).

40
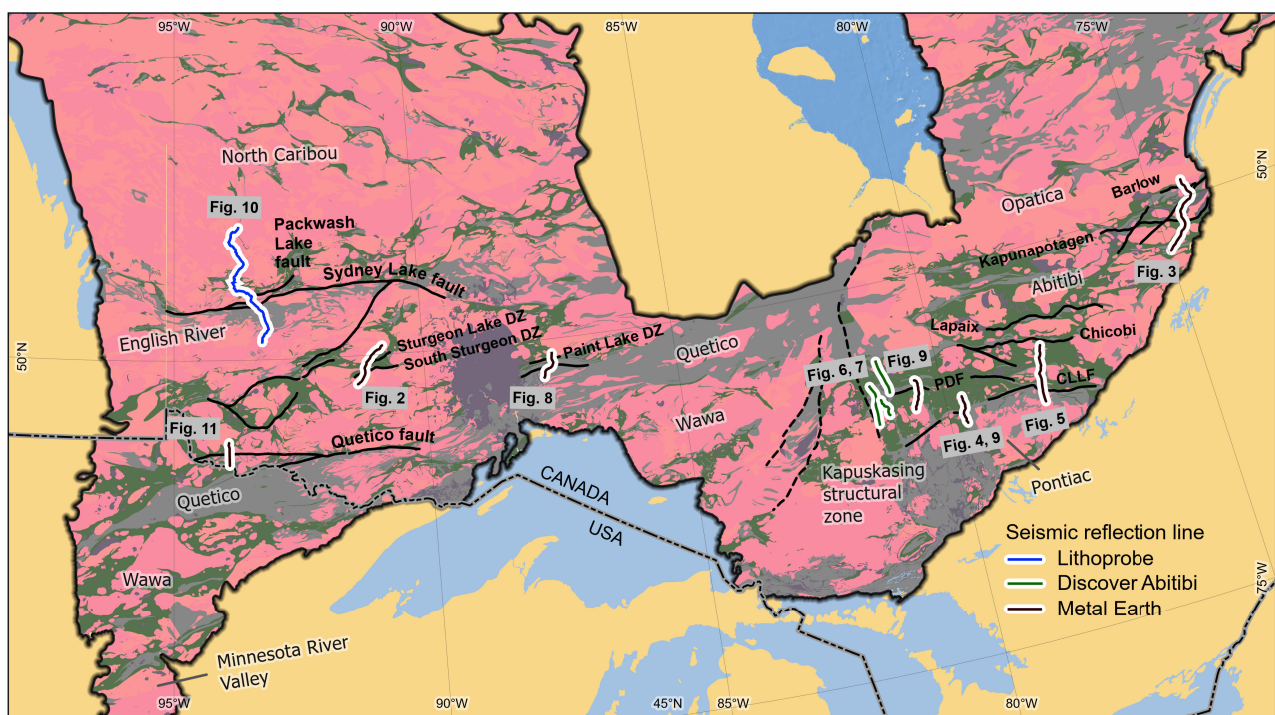
Figure 1: Simplified basement geology map of the southern Superior craton (modified from Percival et al., 2006). Green indicates dominantly mafic greenstone belts, pink granitic plutons and gneiss, and gray metasedimentary rocks. Solid black lines are major faults. Major terranes are labelled but no boundaries are shown as these are disputed and evolving. Locations of seismic reflection profiles used in this study are shown with corresponding figure number. CLL is the Cadillac– Larder Lake fault, PDF is the
45   **Porcupine–Destor fault.**

Seismologists typically consider the crystalline crust as comprising three layers when analyzed using refraction methods or
alternatively, one layer when using receiver functions (Rudnick and Fountain, 1995; Mooney, 2010; Szwillus et al. 2019).
Adopting two or three layers results in good matches between modeled Vp velocities and estimated bulk weight percent SiO_2
50   content (Hacker, Kelemen, and Behn, 2015; Artemieva and Shulgin, 2019). Globally averaged velocities for each layer are
Vp=5.6-6.4 km/s (67 % SiO_2) for the upper crust, Vp=6.5-6.9 km/s (64 % SiO_2) for the middle crust, Vp=7.0-7.4 km/s (53%

Si0$_2$) for the lower crust, and Vp=7.8-8.2 km/s for the uppermost mantle (Mooney, 2010; Hacker, Kelemen, and Behn, 2015).
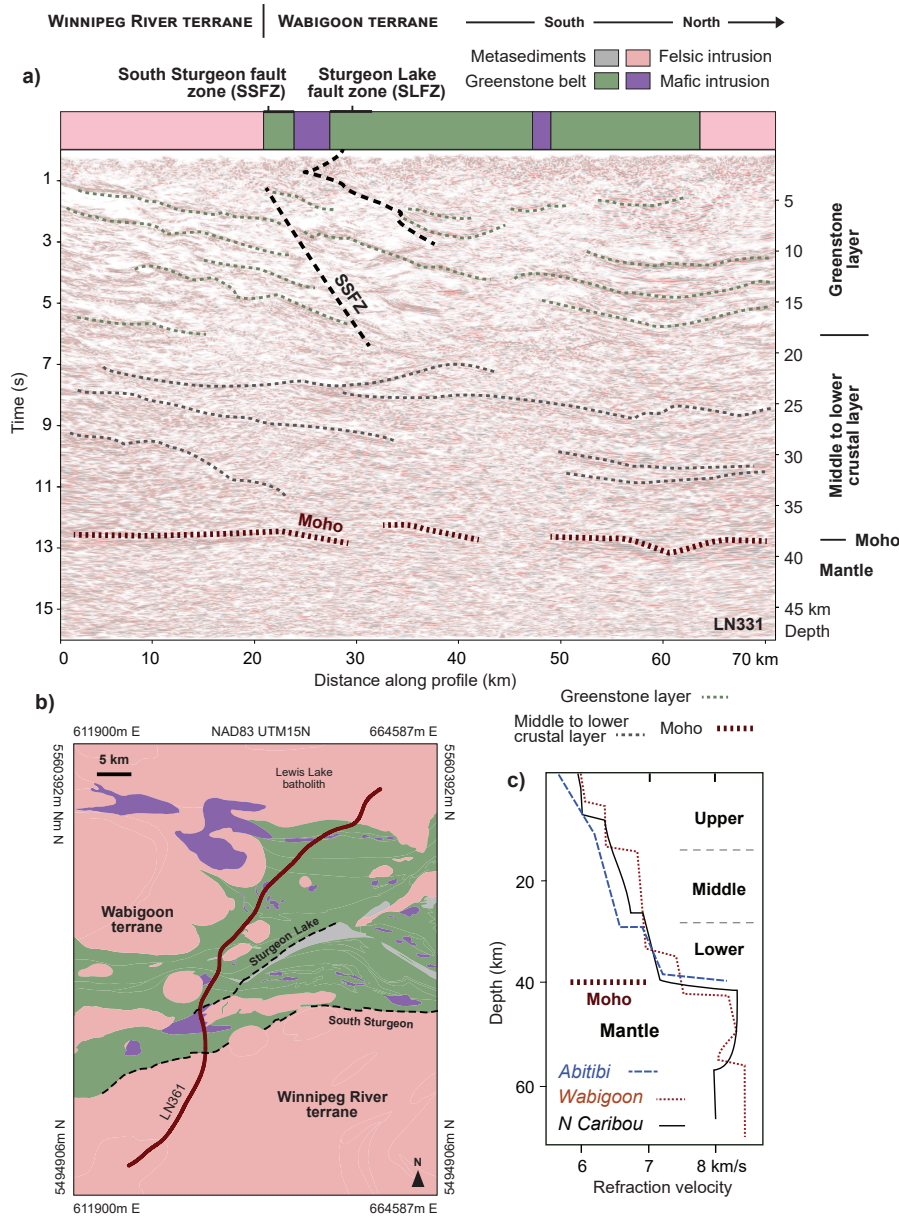
Figure 2: Deep seismic reflection section across the terrane boundary between the Wabigoon and older Winnipeg River terranes: the Metal Earth Sturgeon transect (Figure 1) (Simmons et al., 2024). (a) Strip geology and interpreted seismic reflection section; (b) geological map; (c) seismic wave speed versus depth from near coincident model of Mussachio et al. (2004; Grandjean et al., 1995). Details of seismic data acquisition and processing (prestack migration, curvelet dip coherency enhanced) described in Nazghizadeh et al., 2019).This section illustrates both broad folding and thrusting within the upper crust and layered, gently north-dipping reflectors in the middle crustal layer. Moho at 39-40 km is inferred from crossing seismic refraction models (Musacchio et al., 2004). The South Sturgeon fault zone is the interpreted terrane boundary (Ma et al., 2021).

Similar velocity values are defined for the granite-greenstone terranes of the southern Superior craton (Fig. 2) (Grandjean et al., 1995; Calvert and Ludden, 1999), which have been calibrated by an exposed crustal section at the Kapuskasing uplift

65   (Percival and West, 1994). Variable velocities of 5.6–6.4 km/s characterize the upper crust (0–12 km). a relatively uniform middle crust (~12–30 km) has velocities of 6.4 to 6.6 km/s. A velocity increase of 0.3 km/s occurs at 30–40 km depths, across the middle crust–lower crust boundary. Lower crustal velocities increase from 6.9 km/s to 7.3 km/s at the Moho. Uppermost mantle has velocity of 8.15 km/s. Here we assemble new and older seismic observations (with MT data: Simmons et al., 2024), consistent with previous interpretations of the layered structure of the crust, to constrain the

70   architecture and tectonic history of ancient major faults that cut the crust, and in places the lithosphere, of the Superior craton of central North.

2 Geologic Setting

The upper crustal layer (0–12 km) of the greenstone dominated terranes of Superior craton, which have calibrated velocities

75   of 5.6–6.4 km/s, consists predominantly of ultramafic-felsic volcanic rocks and plutons emplaced between 2.99 and 2.70 Ga (Benn and Peschler, 2005). The preserved volcanic deposits in these terranes record multiple volcanic episodes (assemblages), each characterized by submarine mafic lavas and minor volcaniclastic deposits (± other ultramafic and intermediate to felsic lithologies; Ayer et al., 2002). Within the Abitibi terrane, six Neoarchean metavolcanic assemblages are recognized, defined as the 2750–2735 Ma Pacaud, 2734–2724 Ma Deloro, 2723–2720 Ma Stoughton-Roquemaure,

80   2720–2710 Ma Kidd-Munro, 2710–2704 Ma Tisdale, and the 2704–2695 Ma Blake River assemblages (e.g., Ayer et al., 2002, 2005; Monecke et al., 2017). Their basal contact with 2.87–2.70 Ga tonalitic gneisses lies at 10–12 km depth (Snyder et al., 2008). Eruption of the metavolcanic assemblages occurred coeval with emplacement of syn-volcanic plutons of gabbro and tonalite-granodiorite-trondhjemite (TTG) that form the upper part of the middle crustal layer (Matthieu et al., 2020). The transition from the upper crustal greenstone layer into the middle crustal layer corresponds to an increase in crustal velocities

85   to 6.4–6.6 km/s Grandjean et al., 1995; Calvert and Ludden, 1999). Anorthosite, tonalite, mafic gneiss and paragneiss form layers 0.1 to 10-km thick in the lower part of the middle layer (Percival and West, 1994). The third layer, the lowermost crust, is not exposed but hypothesized to consist of dense, mafic rocks with pyroxene- and amphibole-rich minerals (White et al., 2003; Benn and Peschler, 2005).

Greenstone belts separate plutons and older gneiss domains (Fig. 1). These upper crustal plutonic rocks have generally been

90   classified as syn-volcanic (>2.70 Ga), syn-tectonic (2.72–2.66 Ga), or late intrusions, although some intrusive complexes formed over 90 million years by multiple intrusive events (Ayer et al., 2005; Beakhouse, 2011; Matthieu et al., 2020; 2024). Isotopic zircon dating indicates that syn-volcanic plutons crystallized coeval with the mafic volcanic rocks whereas syn-tectonic plutons typically core folds or crystallized synchronous with formation of sedimentary basins, such as those hosting the English River, Porcupine or Quetico metasediments (e.g., Žák et al., 2023). Late intrusions (post 2.7 Ga) have more

95   hydrous geochemistry and form sanukitoid batholiths and small syenite or pyroxenite bodies (Mole et al., 2021).

Gneissic domains that core terranes of the southern Superior craton include rocks of diverse ages that include the 3.9–2.7 Ga North Superior, the 3.05–2.72 Ga North Caribou/Opinaca, the 3.32–2.66 Ga Winnipeg River (Opatica), the 3.01–2.66 Ga Wabigoon/Marmion, the 2.79–2.69 Ga Wawa/Abitibi, and the 3.5–2.65 Ga Minnesota River Valley terranes (Snyder and Thurston, 2024). These distinct terranes may have accreted successively to the southern margin of the Superior craton

100 (Percival et al., 2012), but Mole et al. (2021) indicate more complexity. Compiled geochronology suggests different pre-2.9 Ga histories for the Opatica, Wawa, Wabigoon, and Winnipeg River terranes; eastern Wabigoon rock ages range from 3.05 to 2.92 Ga with older Winnipeg River ages (>3.30 Ga).
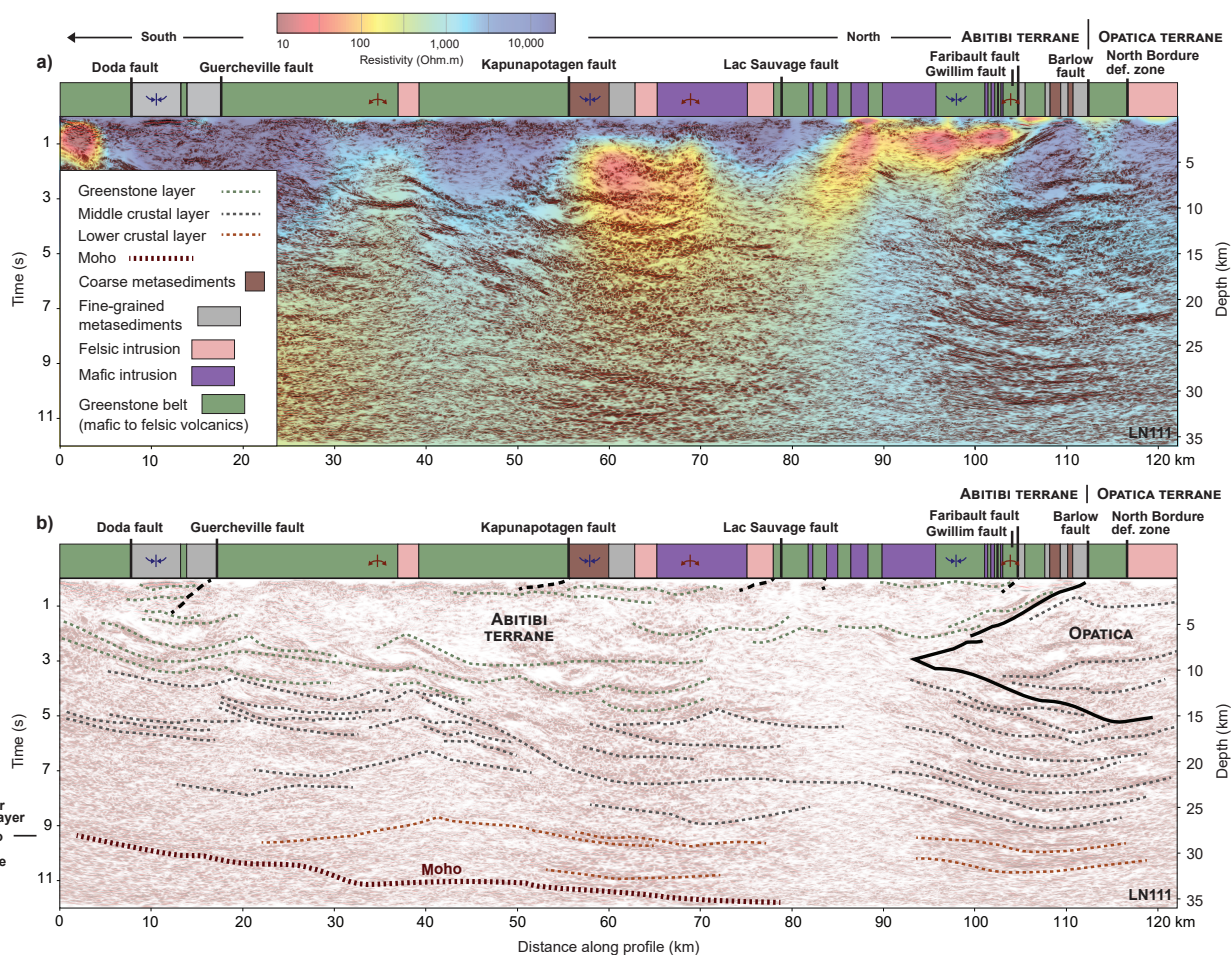
105 **Figure 3: Deep seismic reflection section across the terrane boundary between the Abitibi and older Opatica terranes: the Metal Earth Chibougamau transect (Figure 1). (a) Strip geology, seismic reflection section and conductivity model section (Simmons et al., 2024); and (b) interpreted seismic reflection section. Green, black, red dotted form lines mark upper, middle, lower crustal reflectors, respectively. Heavy dotted line marks interpreted base of Abitibi crustal rocks (Moho). Note step in Moho (red bars) from 38 to 34 km as determined by 3D Ps receiver function analysis (station CHGQ in Snyder et al., 2022). This section illustrates**
110 **both early (D1), broad folding in the upper crust and late-stage (D3) collisional structures in the lower crust underthrusting of juvenile Abitibi crust and wedging of more evolved Opatica (North Caribou) crust between the more juvenile lower crust.**

Dipping seismic reflectors observed on Lithoprobe and more recent deep seismic reflection sections (Fig. 3), which have been interpreted in several locations as lower crust underthrust in a general north direction, permit diverse implied tectonic histories (Calvert et al., 1995; White et al., 2003; Matthieu et al., 2020). This underthrusting thus has been related to serial subduction zones (Percival et al., 2006), subcretion to the leading edge of a drifting proto-craton (Bédard and Harris, 2014) or progressive rifting (Bjorkman, 2017; Mints, 2017; Mole et al., 2021). Many of these interpretations agree that the oldest (Northern Superior) cratonic block began drifting south at ca. 2.72 Ga so that dipping crustal structures record tectonic imbrication ahead of and beneath the drifting proto-continent. One serial subduction model includes at least four subduction zones: North Superioran, Uchian, Shebandowanian, and Minnesotan (Card, 1990).

Mapping has demonstrated that three to five phases of deformation occurred across varied parts of the southern Superior craton (Percival et al., 2006). The cryptic, earliest (D1) phase involves north-south shortening that produced gentle fold interference and sufficient topography to produce widespread sedimentary basins such as those represented by the English River, Quetico and Pontiac sediments and coeval metasedimentary assemblages within the volcanic subprovinces (e.g., the Porcupine assemblage within the Abitibi subprovince). Fold interference patterns imply a second, dextral phase followed relaxation extension (e.g., Davis et al., 1988; Calvert et al. 2004; Bleeker, 2015; Žák et al., 2021; Tóth et al., 2023). The most prominent deformation, the D3 phase of north-south shortening at 2.72-2.66, generally coincided with peak metamorphism and gold mineralization or remobilization (Dubé and Mercier-Langevin, 2020). Later, more localized deformation phases include dextral and sinistral transpressive phases with modest displacements that may represent conjugate shearing (e.g., Bleeker, 2015; Bedeaux et al., 2017; Žák et al., 2021).

Formation of Late Neoarchean metasedimentary belts that host Pontiac, Porcupine, Quetico and English River greywackes indicates that transient uplift and erosion during early (D1-D2) deformation was followed by burial or extensional collapse (Calvert et al., 2004) and then renewed (D3) shortening that culminated in peak metamorphism at 2.69-2.67 Ga (Bleeker, 2015). The latter deformation accompanies distinct (Timiskaming-type) polymict conglomerate and clastic deposits.

The post-2.6 Ga stabilized Superior craton records little subsequent internal deformation with the exception of the Kapuskasing uplift, a 500 km long, east-verging thrust fault-bounded block (Fig. 1) (Percival and West, 1994). Cooling patterns observed within the uppermost 20 km of granulite-facies rocks suggest uplift and rotation of the hanging wall (western) block occurred at about 1.9 Ga (Percival et al., 2012). Paleoproterozoic hydrothermal activity occurred one hundred kilometers to the east, where evidence for quartz veining and possible upgrading of Au deposits suggests incursion of mantle-derived melts at 1.88 Ga and 1.75–1.70 Ga that form part of the Circum-Superior Large Igneous Province (Zhang et al., 2014; Herzberg, 2022).

3 Faults observed on seismic sections: reflections

Determining the geometry of faults at depth requires high-resolution geophysical methods such as seismic reflection profiling. Interpreters generally infer faults from aligned breaks in prominent reflectors, rarely from a continuous reflector

145   itself. Several new data acquisitions relevant to the mapping of faults and related crustal structures have occurred in the southern Superior craton since synthesis of the Lithoprobe program (e.g., Percival et al., 2006; 2012). Crustal-scale and some high-resolution seismic reflection profiling now covers much of the Abitibi and Wabigoon terranes (Simmons et al., 2024). This newer profiling can resolve structures as small as several hundred meters and a kilometer in the upper and lower crust, respectively (Snyder et al., 2008; Nazghizadeh et al., 2019; Haugaard et al., 2021). The Moho and uppermost mantle

150   structures occur deeper than some of these sections, but acquisition of those sections was designed for future reprocessing using extended correlation should deeper images be of particular interest (e.g., Okaya and Jarchow, 1989). New coincident broadband magnetotelluric (MT) soundings along transects augment the mostly long-period MT (LMT) soundings acquired by Lithoprobe (Hill et al., 2021) and provide independent characterization of crustal structures. Three-dimensional analysis and modelling at lithospheric scale of all these data types provides a common reference frame (Snyder et al., 2021).

155   Seismic reflection sections collapse information from a 3-D volume onto a 2-D plane. All crustal reflectors with appropriate strike and dip lying within a triangular prism with an apex axis coincident with the survey line and a base several kilometers wide will appear on the section. Thus, sets of reflectors that appear to cross may lie on opposite sides of the survey line. Careful cross dip analysis and 3-D migration can restore correct geometries but requires considerable processing effort (e.g., Calvert et al., 2004, Cheraghi et al., 2022; Fam et al., 2023). Zones of apparently reduced reflectivity may thus result from

160   either reflectors that occupy only part of the subsurface volume being imaged or changes in rock properties that make rock layers more homogenous or both.

The goal here is to provide a consistent interpretation of recent deep seismic reflection profiles across the southern Superior craton. To that end, selected seismic sections and coincident conductivity sections taken from the Metal Earth Atlas (Simmons et al., 2024) have retained the consistent display parameters and scales. All underlying data were acquired and

165   processed consistently with the exception of the Red Lake and Timmins/Crawchest sections which were acquired in the early 2000's (Calvert et al., 2004; Snyder et al., 2008).

We adopt the traditional interpreted three-layer structure of the Superior craton crust (Bellefleur et al., 1995; Calvert and Ludden, 1999; Benn, 2006; Benn and Peschler 2005; Percival et al., 2012) and use the new reflection/conductivity sections to characterize rock properties and nature of each of these layers in more detail. Our interpretation of the seismic sections

170   (see Fig. 2 or 3 for example) uses form lines to emphasize relatively large amplitude, laterally continuous (minimum several kilometers) reflectors. Green form lines indicate upper crustal reflectors in the presumed brittlely deforming and resistive mafic volcanic rocks of the various Superior greenstone belts. Black form lines indicate reflectors within the presumed plastically deforming and conductive gneiss of TTG composition in the mid-crust; in the Kapuskasing uplift, such reflectivity appears in syn-volcanic and younger plutonic rocks, which were strongly reworked at ca. 2660–2610 Ma into

175   sub-horizontal gneissosity (Percival and West, 1994). Blue form lines indicate presumably strong mafic-ultramafic lowermost crust composed of pyroxenites, amphibolites or garnet granulites. Thick dashed lines map breaks in reflectors and hence the interpreted continuation of named, mapped surface faults at depth. We further assume that greenstones appear

resistive in conductivity models, TTG gneisses appear moderately conductive, and faults are variably conductive (Hill et al.,
2021; Roots et al., 2024).

180 As noted previously, petrogenesis of plutons in the southern Superior craton has historically been distinguished by age as:
(1) synvolcanic with the greenstone mafic lava assemblages (2790–2685 Ma), (2) syntectonic with the major deformation
and metamorphism phase (2685–2667 Ma), and (3) late, during final stages of collision and stabilization (ca. 2.5 Ga
cratonization) of the crust and uppermost mantle (Beakhouse 2011; Ayer et al., 2002; Matthieu et al., 2020, 2024). Tectonic
evolution of major crustal faults will be discussed using the same three-part temporal framework. Particular seismic/MT

185 transects provide the best examples and insights into each crustal layer and thus the faults deforming the crust in each layer

3.1 Syn-volcanic faults

Fault-related structures within the upper crustal greenstone rocks form mainly either steep (>75°) zones of reflector
disruption or low-angle (<35°) thrust faults. Mafic–felsic, juvenile, polycyclic volcanic rocks deposited between 2.99 and
2.70 Ga typically form broad upright folds in greenschist metamorphic facies (Ayer et al., 2002, 2005; Benn and Peschler,

190 2005). The low-angle thrusting, stacking and broad folding of these units clearly post-dates their emplacement. In contrast,
the steep (>75°) zones of disrupted reflectors indicate intermittent faulting synchronous with eruption of the volcanic units.
The contact between resistive greenstone belt volcanic rocks in the upper crust and the more conductive gneissic middle
crust remains controversial. It forms a tectonic boundary if the greenstone belt represents a tectonically emplaced nappe
complex (e.g., Dimroth et al., 1985; Calvert et al., 1995), or a stratigraphic boundary if the volcanic rocks erupted directly

195 onto plutons (e.g., Goodwin & Smith, 1980; Thurston, 2002; Benn & Peschler, 2005).
An example of a steep deformation zone appears most convincingly where the Cadillac-Larder Lake fault zone (Bedeaux et
al., 2017) cuts the 2704–2695 Ma Blake River assemblage near Larder Lake, Ontario (Fig. 4). Individual reflectors or
sequences do not align across the disrupted zone, but also do not indicate uneven vertical movements across the zone. This
suggests largely strike-slip or pull-apart displacements typical of transform faults in modern oceanic lithosphere (e.g., Baxter

200 et al., 2020). The near-vertical fault zones cut reflectors in both the resistive, upper crustal greenstone layer and the more
conductive, layered mid-crustal TTG layer. Eruption of the metavolcanic assemblages occurred in association with
emplacement of syn-volcanic plutons of gabbro and tonalite-trondhjemite-granodiorite. Many of these near-vertical fault
zones may thus be very long-lived, with multiple reactivations in diverse stress regimes. The Peggy Ridge fault in the Lau
Basin in the southwest Pacific Ocean may represent a modern analogue of such faults (Baxter et al., 2020). Many of these

205 steep deformation zones have relatively high conductivity that varies along strike and thus represents a strongly 3-D
conductivity structure.
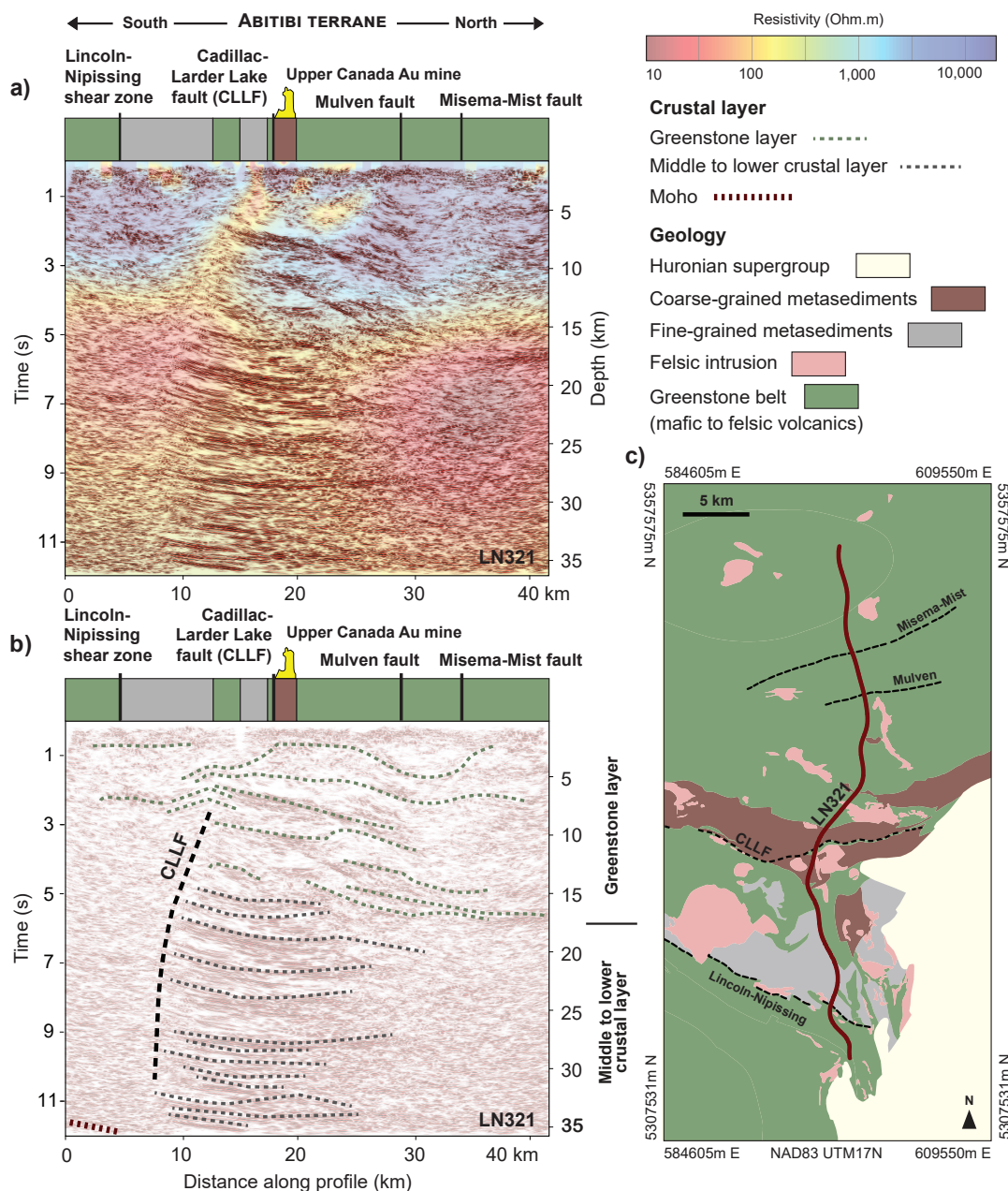
Figure 4: Deep seismic reflection section across the Cadillac–Larder Lake fault zone in the central Abitibi terrane: the Metal Earth Larder Lake transect (Fig. 1). (a) Strip geology, seismic reflection section and conductivity model section (Simmons et al., 2024); (b) interpreted seismic reflection section; (c) Geologic location map. This section illustrates strongly layered reflectors (dotted black form lines) throughout much of the (middle) crustal layer. Moho at 38-40 km estimated from a coincident Ps receiver function transect (Nazghizadeh et al., 2022). Interpretation of some shallow (< 2 km) reflectors benefited from cross-dip analysis (Fam et al., 2023).

3.2 Syn-tectonic faults

Late Neoarchean metasedimentary belts within the Superior craton (e.g., English River, Quetico, Porcupine and Pontiac greywackes) record erosion during early (D1) shortening, extensional collapse about 2.75 Ga (Calvert et al., 2004) and renewed (D3) shortening culminating in peak metamorphism at 2.69-2.67 Ga (Mueller and Donaldson 1992; Leclerc et al. 2012; Bleeker, 2015; Matthieu et al., 2020).
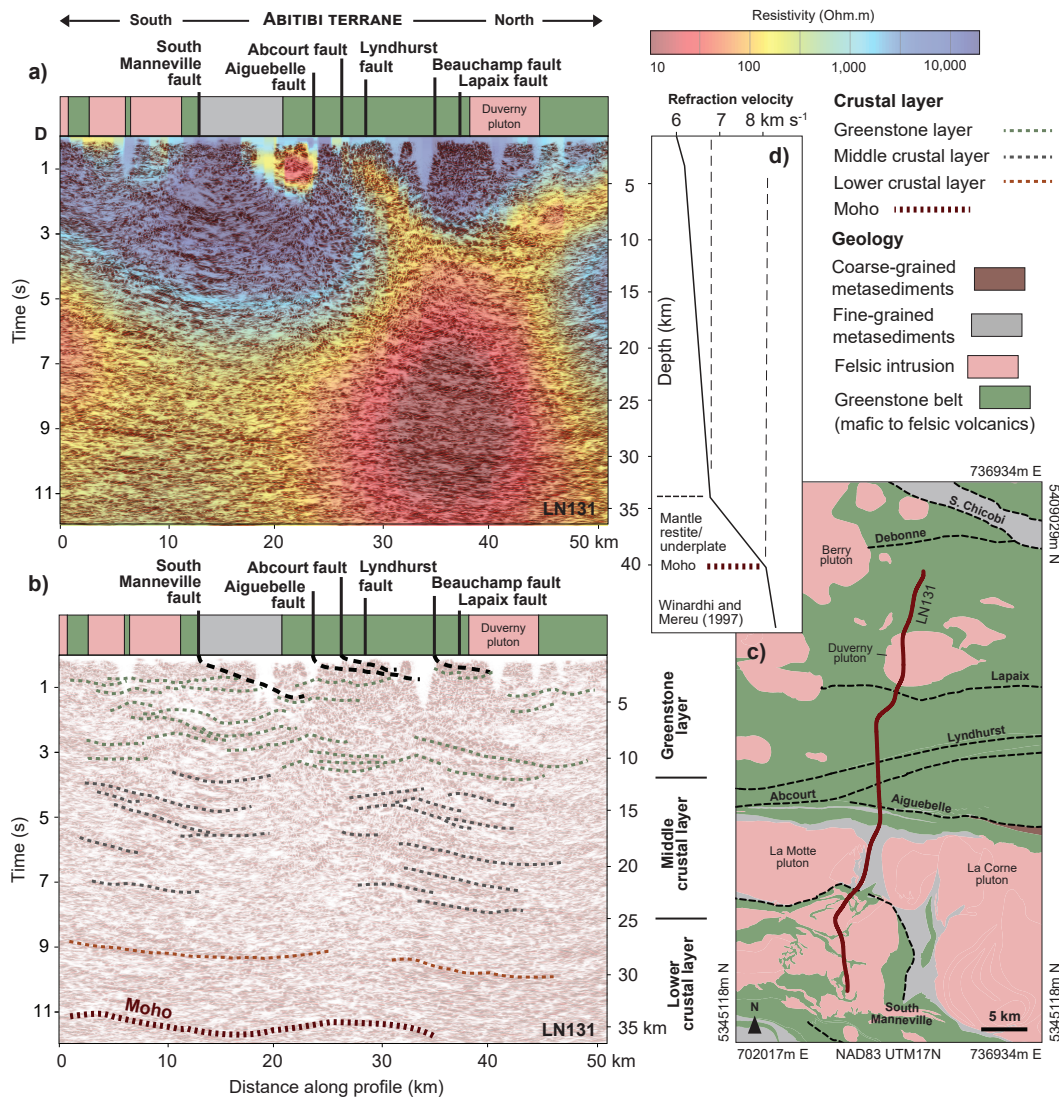
Figure 5: Deep seismic reflection section across the central Abitibi terrane: the northern part of the Metal Earth Malartic transect (Fig. 1). (a) Strip geology, seismic reflection section and conductivity model section (Simmons et al., 2024); (b) interpreted seismic reflection section; (c) Geologic location map; (d) Velocity-depth profile (Calvert & Ludden, 1999). Seismic data processed as in Fig. 2. This section illustrates both broad folding and thrusting within the upper crust and strongly layered reflectors in the middle crustal layer. Moho at 38-40 km is inferred from seismic refraction models 50 km to the north (Grandjean et al., 1995).

Low-angle faults observed within greenstone belts across the Superior craton fold and stack the preserved metavolcanic and metasedimentary assemblages indicating that they were active after eruption of the volcanic rocks (Figs. 5–9). Folded and

230   thrust-stacked greenstone belts across the southern Superior craton occupy the upper crust to 10–25 km depth, based on their consistently high resistive character and a decrease in reflector density beneath the inferred basal intrusive or fault contact between the greenstone assemblages and 2.87–2.70 Ga tonalitic gneisses of the middle crust (e.g., Snyder et al., 2008).
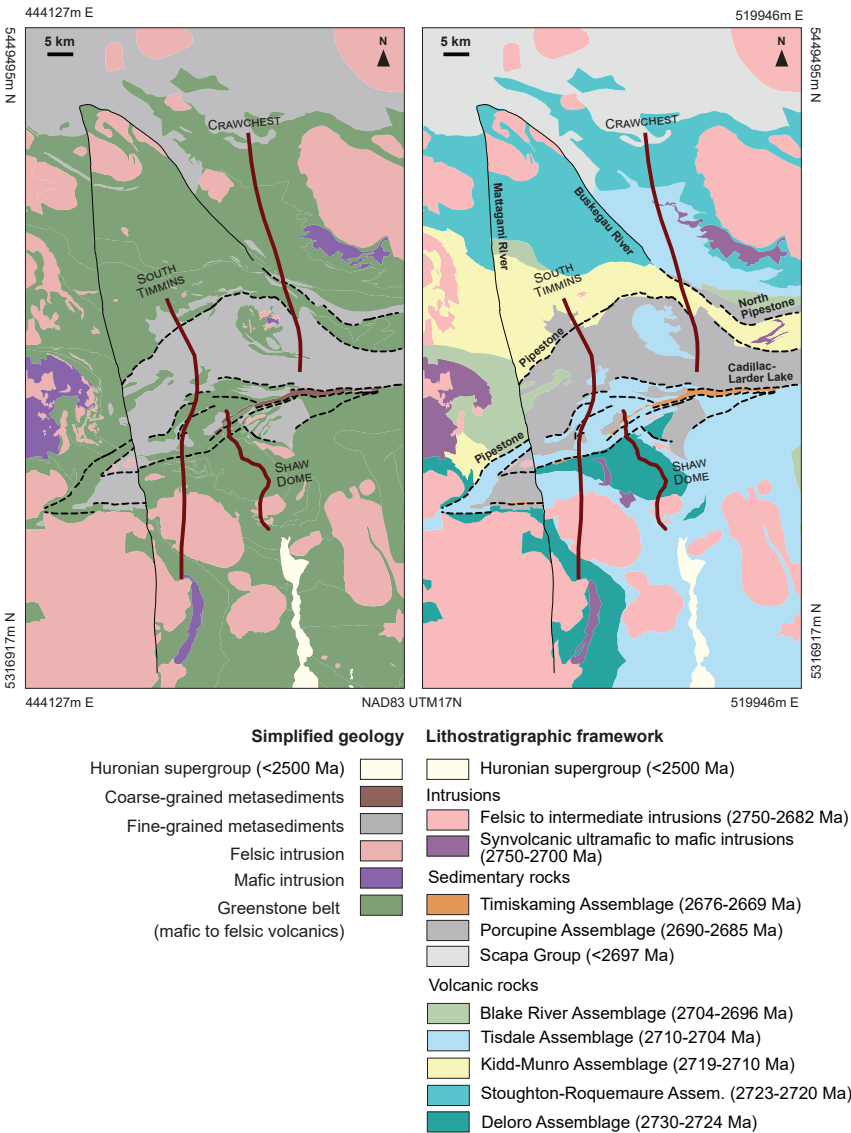
235   **Figure 6: Geological and assemblage (lithostratigraphic) maps for Crawchest and South Timmins transects (Simmons et al., 2024).**

Intense geological investigations around the Timmins-Porcupine mine camp (Fig. 6) provides sufficient information of the greenstone assemblage thicknesses and deformed geometries (e.g., Ayer et al., 2005; Snyder et al., 2008) to permit approximate palinspastic restoration of the original sections (Fig. 7). Mapping demonstrates that the folds and thrusts in this

240 area are 3-dimensional, but a majority of cumulative horizontal shortening was north-south oriented (Bleeker, 2015), thus broadly parallel to the orientation of the chosen cross section constrained by seismic reflectors. One permissible restoration (Fig. 7) indicates about 40 km of north-south shortening within the greenstones and metasediments during the early-D3 phase of south-verging, thin-skinned thrusting on a family of thrust faults related to the low-angle Pipestone fault (Bleeker, 2015; Haugaard et al., 2021). A lesser amount of shortening occurred immediately to the south during north-verging, thick-

245 skinned thrusting on thrusts related to the Porcupine-Destor fault (Figs. 7, 8) (Adetunji et al., in review).
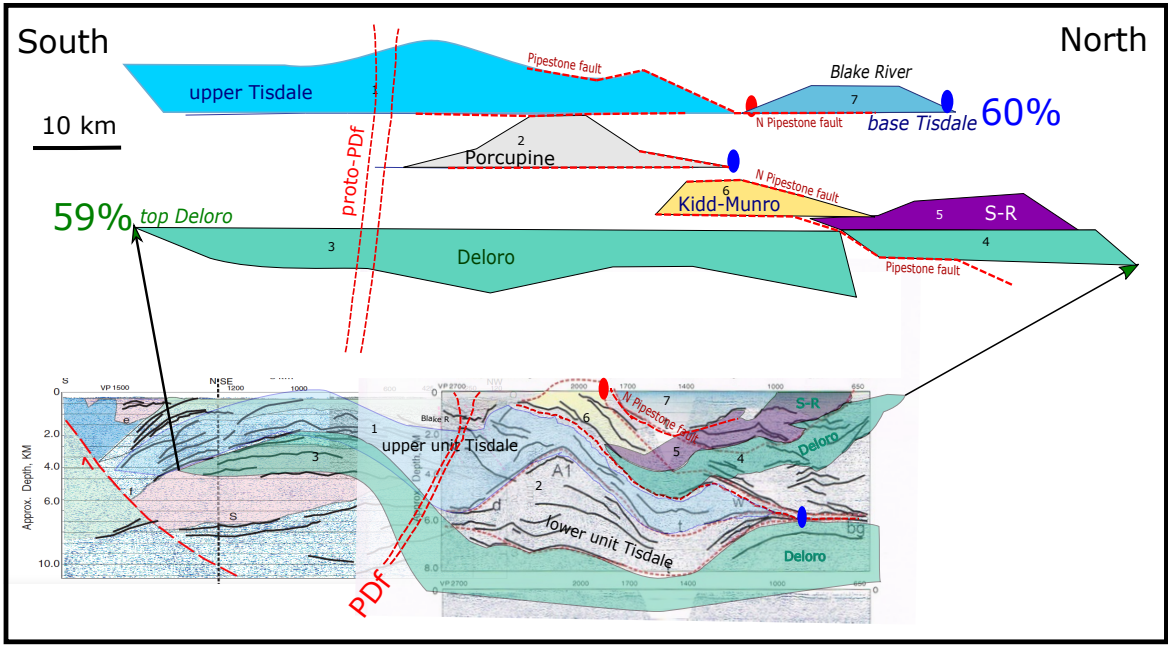
Figure 7: Crawchest geologic cross section: palinspastically restored (a) and interpreted (b) based primarily on Snyder et al. (2008) with their seismic sections shown. Corresponding assemblage names (e.g., Tisdale), numbered tectonic blocks (e.g., 2) and piercing
250 **points (upright blue ovals) are indicated in both a and b. Estimated horizontal lengths at two assemblage contacts indicate final length has about 60% of the length of the original. PDf is the Porcupine–Destor fault zone.**
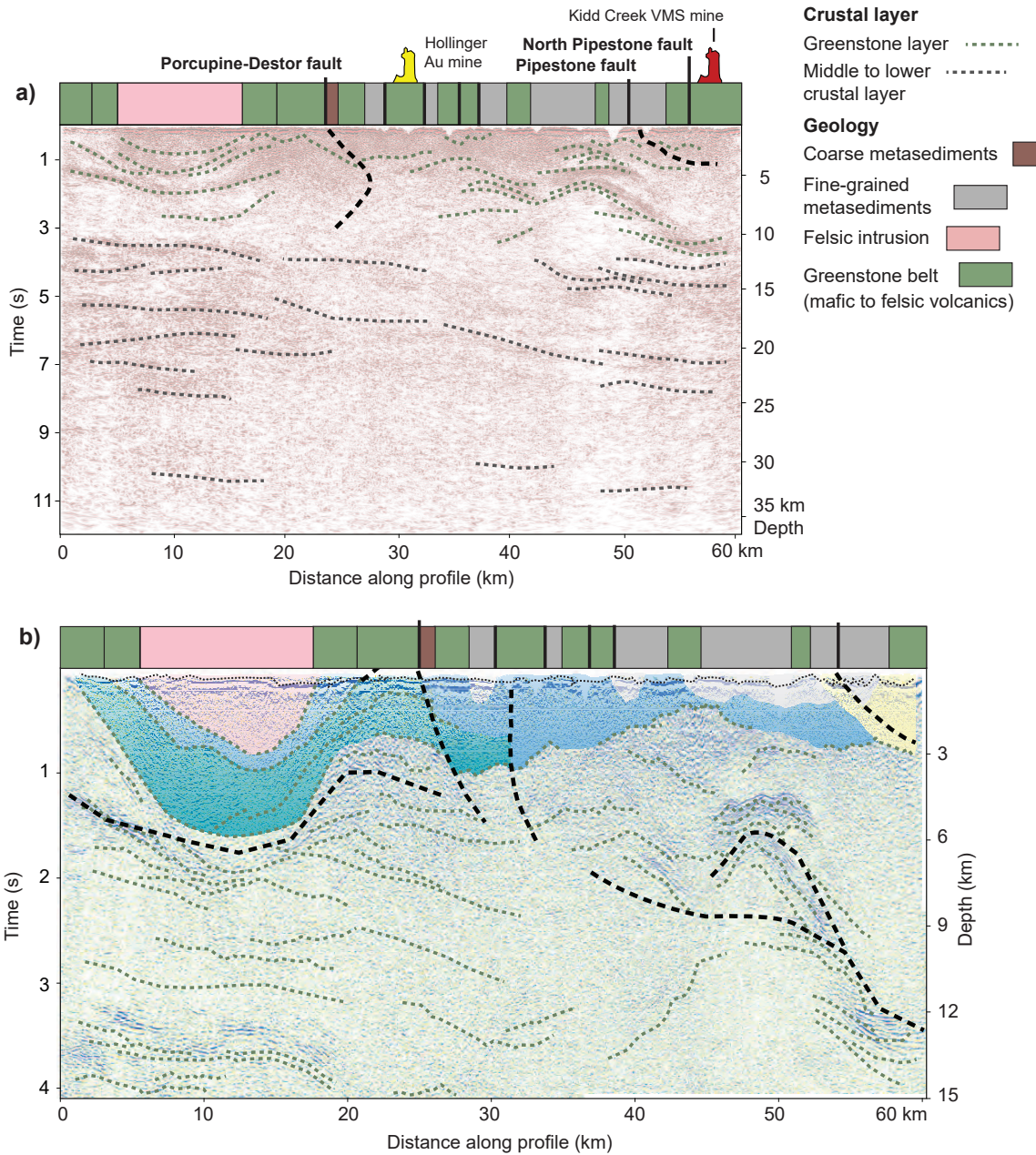
Figure 8: Deep seismic reflection section across the Porcupine–Destor fault zone and Timmins gold camp of the Abitibi terrane: the Metal Earth South Timmins transect (Fig. 1). Location map is Fig. 6. (a) Strip geology and interpreted seismic reflection section (Simmons et al., 2024); and (b) detailed interpreted seismic reflection section of upper crust (Snyder et al., 2008). This section illustrates strongly layered reflectors (dotted black form lines) throughout much of the (middle) crustal layer beneath thrust and fold belt greenstones.

255
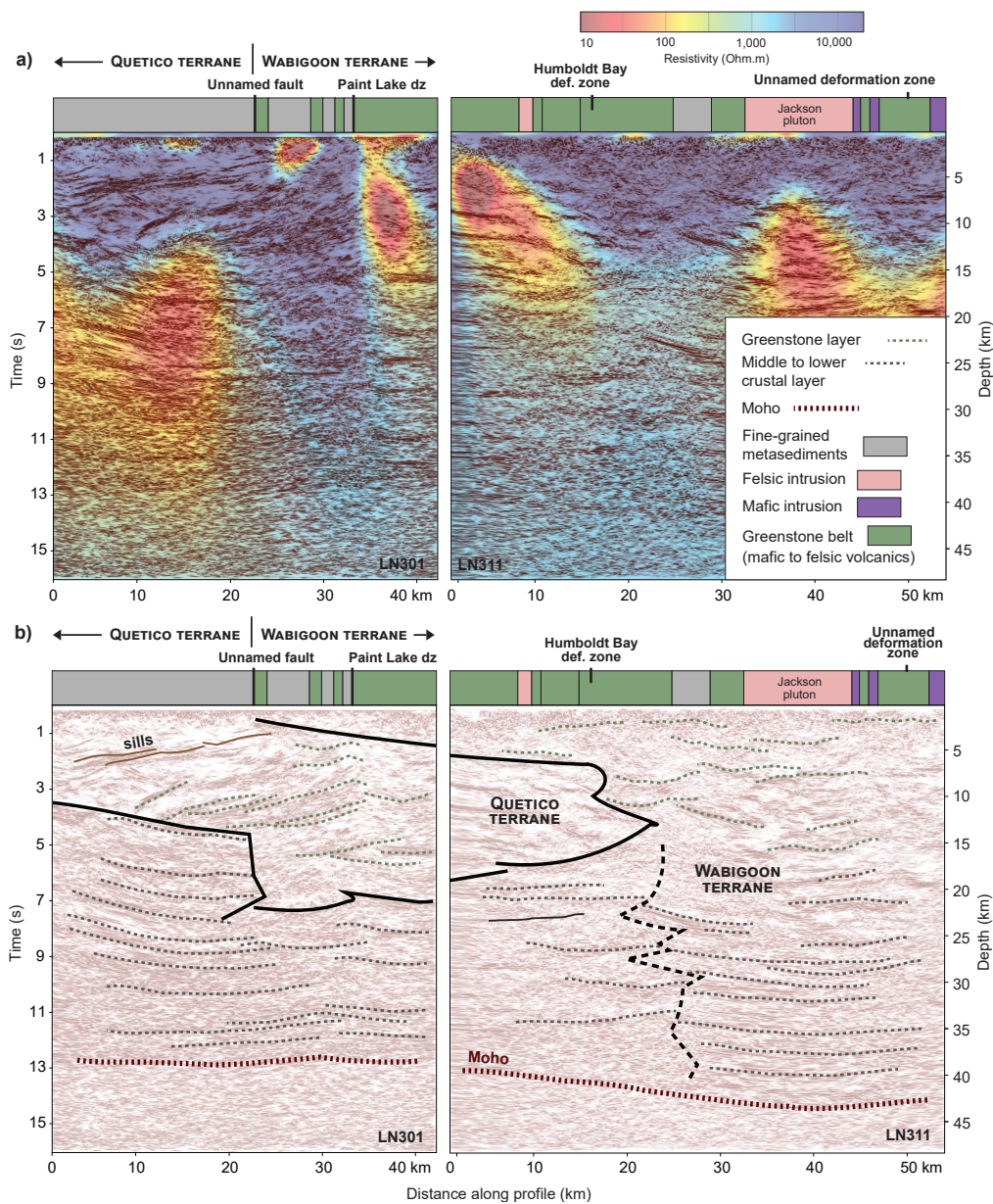
Figure 9: Deep seismic reflection section across the Beardmore-Geraldton Belt: the southern part of the Metal Earth Geraldton transect (Fig. 1). (a) Strip geology, seismic reflection section, and conductivity model (Simmons et al., 2024); and (b) interpreted seismic reflection section. This section illustrates thrusting/wedging within the uppermost crust of the Wabigoon terrane southward over Quetico metasedimentary rocks and layered, gently north-dipping reflectors in the middle crustal layer of the Wawa terrane. Moho at 38-40 km is inferred from 3D Ps receiver function analysis (station GTO in Snyder et al., 2022).

About 50 km to the east in the Matheson area (Fig. 1), drilling and seismic section interpretation indicate that, regionally, the Porcupine-Destor fault dips about 30-40° to the south whereas the south verging Pipestone thrust coincides at the surface with the north boundary of Porcupine assemblage and dips to the north (Snyder et al., 2008; Haugaard et al., 2021). These thrusts can be identified using seismic reflectors within the upper crustal greenstone layer, but not so clearly within the mid-crust (Fig. 8). Steeply south-dipping zones of increased conductivity and disrupted or highly attenuated reflections at 15-30 km depths observed on several geophysical transects suggest continuation of the thick-skinned faults at depth (Haugaard et al., 2021). Although crustal conductivity proximal to the Porcupine-Destor fault is three-dimensional and heterogeneous, the footwall generally appears more conductive and can help map the fault at depth (Fig. 10b). Further east, near the Larder Lake transect, passive seismic studies identified a prominent seismic discontinuity dipping about 30° to the south immediately beneath the Moho (Fig. 10a). This Ps seismic discontinuity may represent a yet deeper continuation of the Porcupine-Destor fault that was displaced/offset from its shallower segments (Naghizadeh et al., 2022).
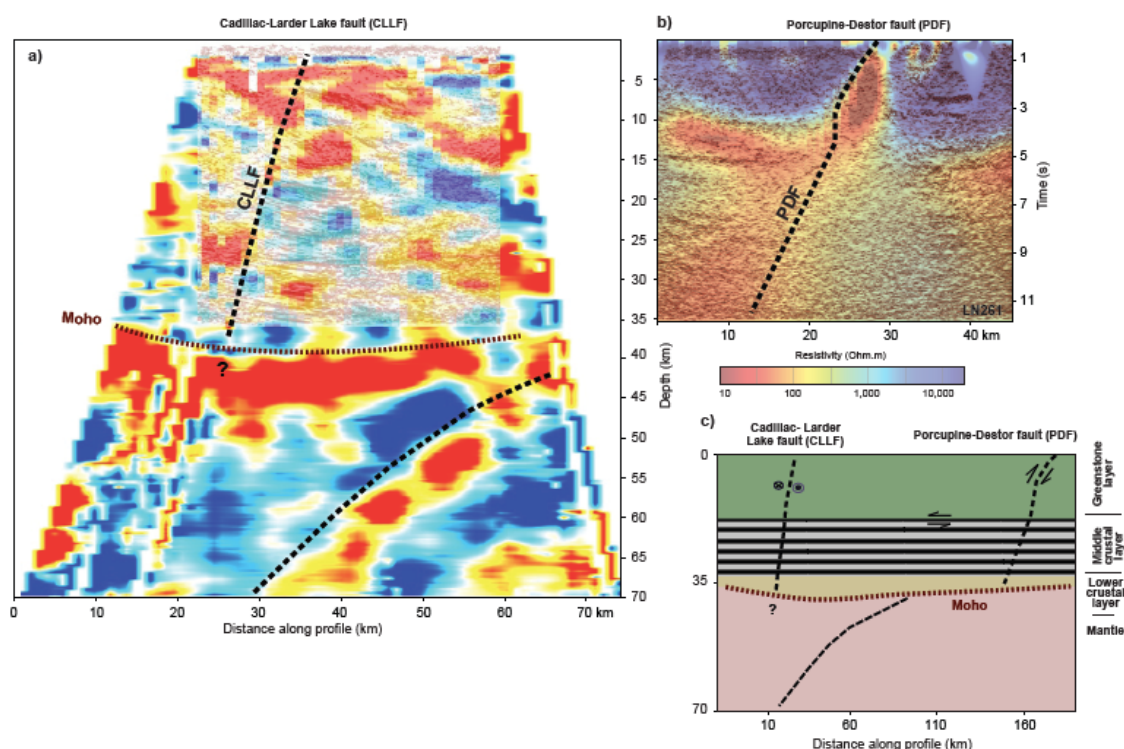
Figure 10: (a) a P-S convertibility section for the Larder Lake transect from receiver function analysis of the passive seismic data (Naghizadeh et al., 2022). This image is an average of all the frequency bands. Hotter colors are positive convertibility amplitudes and cooler colors are negative. CLLF is the Cadillac-Larder Lake fault zone. (b) seismic reflection section and conductivity model of the Metal Earth Matheson transect (Simmons et al., 2024). (c) Structural interpretation of P-S section using several nearby seismic reflection sections for a more regional context. Sense of displacement shown is for peak D3 strain, all of these faults experienced displacements with the opposite sense before or after D3.

Further to the east, a seismic section north of the Malarctic gold mine and Cadillac-Larder Lake fault zone (CLLF) (Bedeaux et al., 2017) helps to project several surface faults at depth: the South Manneville, Aiquebelle, and Abcourt faults all appear as low-angle faults within the greenstone rocks of the Blake River assemblage (Fig. 5). Conductors suggest that some

290 continue as fractures into the mid-crust. The overall northward dip suggests that these faults form a family of structures more akin to the Destor-Porcupine and Pipestone faults rather than to the CLLF.

In the Wabigoon terrane a seismic section across the Beardmore-Geraldton Belt (Fig. 1) shows a trio of low-angle thrusts where greenstones of the Wabigoon terrane are thrust southward and imbricated with more conductive metasedimentary rocks of the Quetico basin (Fig. 9). This thrusting again represents D3 north-south shortening observed across the Superior

295 craton (considered D2 by Tóth et al., 2023). Its extent into the mid-crust suggests the belt represents a significant southern boundary of the Wabigoon terrane.

3.3 Terrane boundaries & Moho offsets

Surface faults that penetrate the lower crustal layer are rare (Stern and McBride, 1998). This layer is largely defined by its relationship to the Moho discontinuity. Reflection profile sections seldom unambiguously define the Moho but do enable

300 assessment of the lowermost crustal layer (Cook et al., 2010). Interpretations of several Lithoprobe seismic reflection sections within the Superior craton identified reflections dipping at low angle from the lowermost crust into the uppermost mantle, creating a step in the inferred Moho depth (e.g., Calvert et al., 1995; White et al., 2003; van der Velden and Cook, 2005). In addition to two Lithoprobe refraction surveys (Grandjean et al., 1995; Musacchio et al., 2004), isolated teleseismic stations (Frederikson et al., 2007; Schaeffer and Lebedev, 2014) provide sparse multi-azimuthal estimates for Moho depth

305 across the central Superior craton, ranging from 34 to 47 km depths (Snyder et al., 2021). Teleseismic stations near the Quetico/Porcupine basins have associated Moho depth estimates greater than 44 km; stations to the north and south generally have Moho depths of 39 to 42 km, values typical of Archean crust worldwide (Abbott and Mooney, 2013). The estimates greater than 44 km thus suggest thickened crust along a linear tectonic feature such as a major terrane boundary.

Seismic reflection profiles across the southern Superior craton have also been interpreted to indicate similar local Moho

310 topography of a few kilometers. Shallowly north-dipping reflectors in the middle and lower crust characterize these seismic sections that cross terrane boundaries between juvenile and older (with respect to 2.7 Ga) terranes. Such north-dipping reflectors occur near the Moho in the eastern Superior craton beneath the Abiitibi-Opatica terrane boundary (Fig. 1) (Calvert et al., 1995; Matthieu et al., 2020; Daoudene et al., 2022). Near Chibougamau, the Barlow – North Bordure faults appear to form the terrane boundary (Fig. 3). Prominent southward dipping reflectors in the upper crust combined with northward

315 dipping reflectors throughout the mid- and lower crust define an overall crustal wedge geometry. The 2.82-2.70 Ga Opatica crust wedges apart the 2.75–2.70 Ga Abitibi crust (Fig. 3b). The hanging wall block of the Barlow fault has much greater conductivity than its footwall (Fig. 3a).
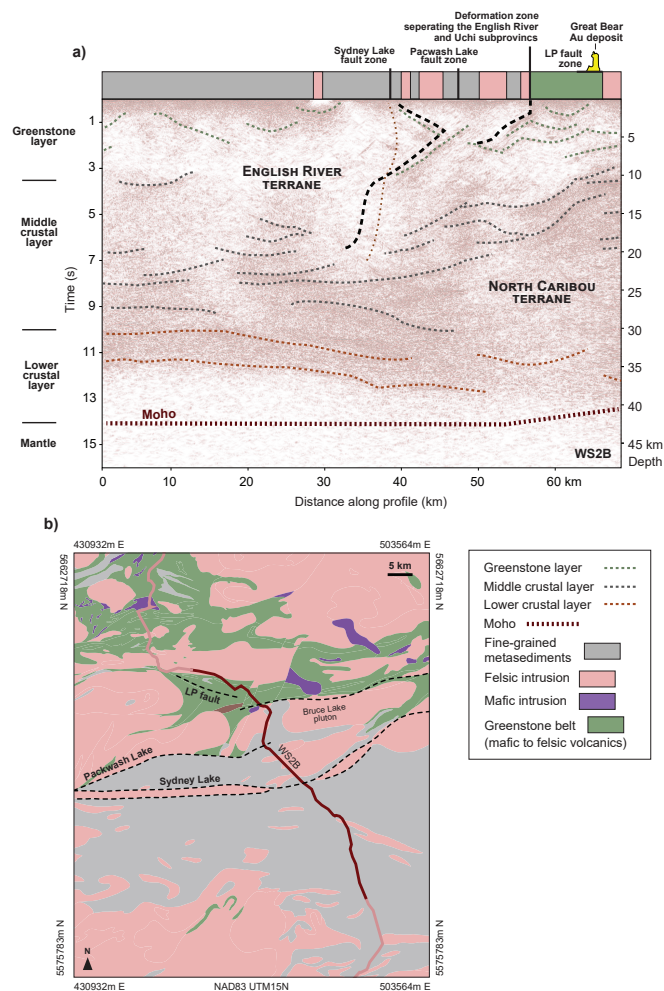
Figure 11: Deep seismic reflection section across the terrane boundary between the North Caribou terrane and English River basin: the central part of the Lithoprobe Western Superior line 2B (Fig. 1). (a) re-interpreted seismic reflection section; (b) geological location map. Seismic section and Moho as described in Calvert et al. (2004). The Sydney Lake fault is interpreted to mark the terrane boundary.

Near Sturgeon Lake in the western Superior craton, similar reflectors occur beneath another terrane boundary (Fig. 2). These features have been interpreted as subduction, or at least underthrusting, of the southern 3.5–2.26 Ga Winnipeg River terrane beneath its northern neighbor, the 2.77–2.71 Ga Wabigoon terrane (Sanborn-Barrie and Skulski, 2006; White et al., 2003, Ma et al., 2021). Here an ambiguous Moho offset coincides with a marked change in seismic velocities within the lower crustal layer (Mussachio et al., 2004). The South Sturgeon and Sturgeon Lake faults, 200 km to the southeast, represent the upper crustal terrane boundary between the Winnipeg River and Wabigoon terranes (Percival et al., 2012). The Sturgeon Lake fault was interpreted previously by Ma et al. (2021) to cut vertically through the entire crust and to offset a horizontal reflector interpreted as the Moho. Our new alternative interpretation of a moderately northward dipping geometry is based on

the lack of steeply aligned truncations of reflectors anywhere within the zone between the Sturgeon Lake and South Sturgeon faults (Fig. 2). In 3D, a large lower-crustal conductor runs parallel to Sturgeon Lake fault zone and projects into the upper crust where the two faults intersect.

335
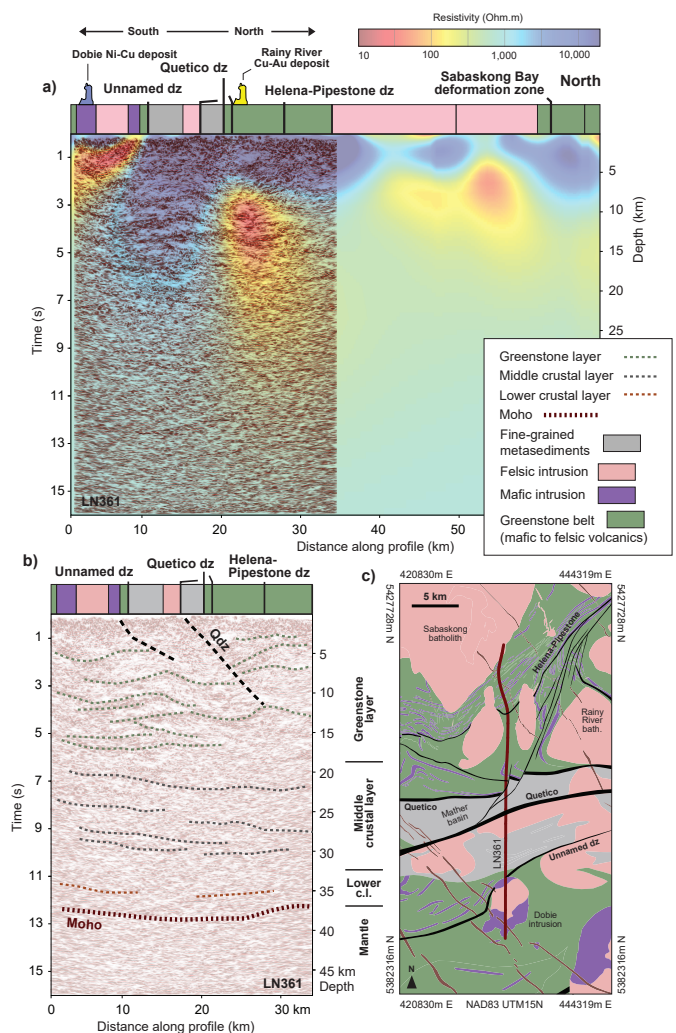
Figure 12: Deep seismic reflection section across the terrane boundary between the Wabigoon and Quetico terranes: the Metal Earth Rainy River transect (Figure 1). (a) Strip geology, seismic reflection section and conductivity model section (Simmons et al., 2024); (b) interpreted seismic reflection section; (c) Location geological map. This section illustrates broad folding and thrusting within the upper crust and layered reflectors in the mid- to lower crust. Moho at 37 km is inferred from regional seismic refraction
340 **models (Musacchio et al., 2004). Qdz is the Quetico deformation zone, the interpreted terrane boundary (White et al., 2003).**

About 50 km to the north, the Sydney Lake fault forms the terrane boundary between the Uchi subprovince of the North Caribou terrane and the Winnipeg River terrane, here covered by the English River basin (Fig. 1) (Hrabi and Cruden, 2006; Hynes and Song, 2006; Percival et al., 2012). Calvert et al., (2004) previously interpreted a nearly vertical fault geometry within the upper crust that ends at a gently south-dipping horizontal reflector at 20 km depth (dashed orange line in Fig. 11).

Our new interpretation of wedge geometries relies on the presence of angularly intersecting reflectors and a lack of steeply
aligned reflector truncations beneath the surface fault zone.

The Quetico fault, 300 km to the southwest, forms a terrane boundary between the Wabigoon and Quetico terranes near
Rainy River, Ontario (Figs. 1 and 12) (Percival et al., 2012; Hendrickson, 2016). Another segment of the Quetico fault, 250
km to the east, was interpreted previously as cutting nearly vertically within the upper half of the crust and bottoming at a
gently north-dipping reflector defining the lowermost crust (White et al., 2003). Our alternative interpretation of moderate
northward dipping geometry, consistent with the Beardmore-Geraldton Belt interpretation (Fig. 9), notes the lack of
vertically aligned truncations of reflectors within the inferred greenstones and Quetico basin metasediments that underlie the
Quetico fault zone here (Fig. 12). Hendrickson (2016) modeled aeromagnetic data that he used to interpret a broad, steep-
sided (~80) synform structure to the Quetico basin within the uppermost 5 km of the crust. The inferred steep banded iron
formation and mafic units may border the Quetico fault in the top few kilometers where incompletely migrated (in 3D)
reflections lie, but near-horizontal reflectors at 4–10 km depths appear more reliable indicators of structure within the
Quetico basin (Fig. 12).

3.4 Late or post-tectonic fault displacements

Late (2.665–2.595 Ga) movements on faults across the southern Superior craton vary locally from area to area but
generally have strike-slip displacements that appear to accommodate continuing, lesser amounts of north-south shortening
(Percival et al., 2012; Bleeker, 2015; Bedeaux et al., 2017; Dubé and Mercier-Langevin, 2020). Remobilized gold and
sulfides, sanukitoid plutons, two-mica granites, and small syenite or pyroxenite bodies all indicate a significantly more
hydrous geochemistry (Mole et al., 2021) and voluminous inferred fluid movement through fault zones (Hill et al., 2021;
Roots et al., 2022). Few fault displacements of this type have been recognized uniquely on Metal Earth seismic reflection
sections, probably because these (D4 & D5) displacements are relatively small compared to the main (D3) north-south
shortening strains.

A boundary between the Abitibi and older Opatica terranes occurs in the Timmins area (Daoudene et al., 2022), but
a proposed boundary marker, the Buskegau fault strikes NNW/340 whereas the recognized regional terrane boundary strikes
ENE/070 (Fig. 6b). A wedge of metasedimentary rocks interpreted locally based on seismic reflections and 3-D conductors
(Fig. 7) probably has associated deeper wedging of mid- and lower crust based on interpretations of seismic transects that
cross this terrane boundary further to the east (Bellefleur et al., 1995; Calvert et al., 1995; Calvert and Ludden, 1999). The
Buskegau fault is a NW-trending late Archean fault which has significantly modified the distribution of Abitibi greenstone
belt assemblages north of the Pipestone fault (Fig. 6).

4 Implications of these observations

375   Aligned offsets and local topography on the Moho suggest that only two lithospheric scale tectonic boundaries, perhaps sutures, occur within the southern Superior craton. Based on the location of Moho offsets, possible sutures coincide with the southern boundary of the North Caribou terrane (Calvert et al., 2004) and the northern boundary of the Abitibi terrane (Calvert et al., 1995). In the southwestern Superior a series of micro-continental, crust-only terranes (Winnipeg River, Wabigoon, Marmion) lie between these main boundaries and above a SE-dipping mantle seismic discontinuity (Snyder and

380   Thurston, 2024), a tectonic setting similar to the present-day western Pacific (e.g., Macpherson and Hall, 2002) or the Mesozoic Pacific northwest of North America (Colpron et al., 2007). The southeastern Superior has only the Opatica and Abitibi terranes and this simplification may indicate the absence of microcontinents and that the main boundaries merge in the east (Daoudene et al., 2022). Next, we explore fault specific implications of these large-scale tectonic trends.

4.1 Restoration of major fault geometries

385   Reconstructing relatively late deformation to remove associated strain and displacements makes it possible to recreate geometries of major faults before these displacements. Palinspastic restorations of the 2.72-2.66 Ga fold and thrust belt in the Timmins area (Dubé, and Mercier-Langevin, 2020) and estimated rotation on the Kapuskasing structure between 2.07 and 1.87 Ga (Evans & Halls, 2010) represent late deformations that affected the Superior craton (Fig. 13). Younger regional-scale deformation, other than dyke intrusions, has not been recognized.

390   The D3 phase of north-south shortening at 2.72-2.66 represents most of the crustal deformation recognizable today in the southern Superior (Dubé, and Mercier-Langevin, 2020). Structural measurements spanning the craton indicate a consistent D3 north-south horizontal shortening with systematic and slight deviations near major high-strain zones (e.g. Hrabi and Cruden, 2006; Bedeaux et al., 2017; Tóth et al., 2023). Benn (2006) argued that north-south shortening occurred via localized intense folding and flattening in the upper crustal greenstones, pure shear in the weaker mid-crustal TTG gneisses,

395   and large-scale imbrication in the stronger pyroxenite-peridotite rocks of the lowermost crust and uppermost mantle (e.g., Fig. 3). A detachment surface between basal greenstones and basement gneisses would be needed to accommodate differential strain locally, and prominent basal reflectors at 10–25 km depths are often interpreted as this boundary zone (Fig. 7) (Benn and Peschler, 2005; Snyder al., 2008).

Both of these recognized deformations directly affect the two main shear zones internal to the Abitibi terrane: the Cadillac-

400   Larder Lake (CLLF) and Porcupine- Destor (PDF) shear zones (Fig. 1). Restoring the rotation and horizontal shortening described above makes these faults more linear and parallel to each other in map view (Fig. 13a). In cross section (Fig. 13b), the south-dipping PDF and near-vertical CLLF geometries inferred from our seismic sections form paired, partitioned strain structures (Fig. 10b) typically found in convergence zones where the dipping fault absorbs boundary-normal shortening, the vertical fault oblique strains (e.g., Tikoff and Teyssier, 1994; McCaffrey, 2009; Haq and Davis, 2010), here at lithospheric

405   scale. This unique lithospheric-scale strain partitioning may result from the inferred syn-volcanic origin of this pair of faults.

We did not recognize similarly paired structures in other seismic sections discussed here, but wedge geometries appear commonly at recognized major terrane boundaries (e.g., Figs. 3, 9 and 11). Inferred underthrusting of only a few tens of kilometers of the Moho in these locations implies that even less horizontal shortening occurred within neighboring crust. Thus, neglecting any former thin lithosphere that is now no longer observed, little additional deformation can be recognized

410   for restoration.
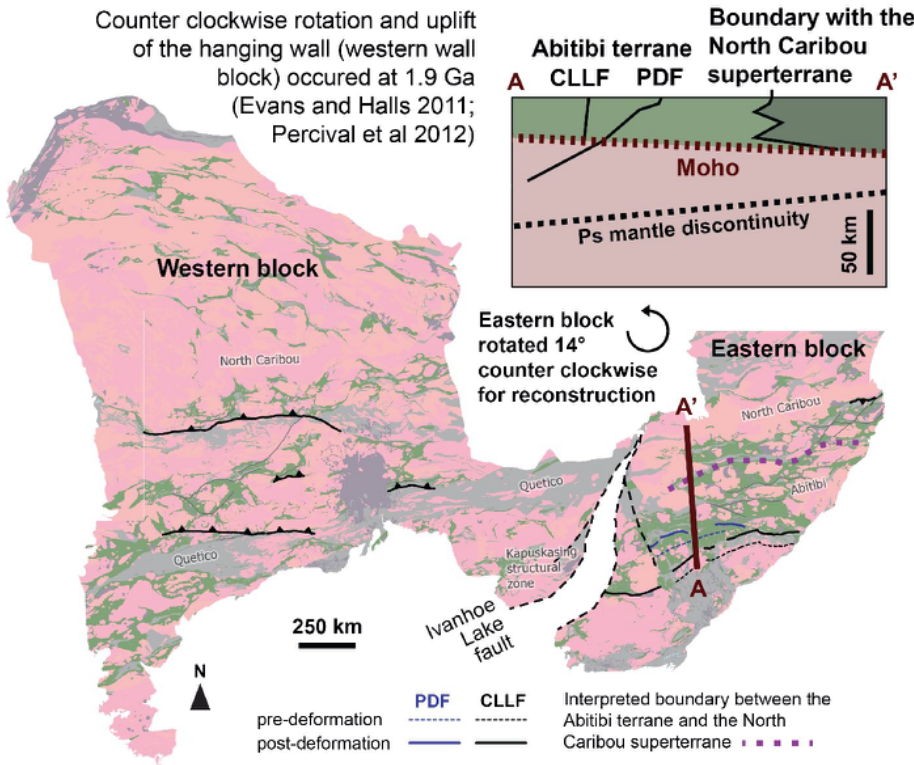
Figure 13: Reconstructed fault geometries in map view, and in a north-south schematic cross section. The map shows a restoration of the eastern Superior relative to a 'pinned' western part about an Euler pole at 51°N, 85°W; with a rotation angle of 14° CCW.
415   **Distributed shear of 90 km of dextral transpressional displacement at ca. 1.90 Ga manifested half as distributed strain within the Ivanho Lake fault and half as oblique lateral thrusting (with NE-vergence) across the Ivanhoe Lake shear zone (Evans & Halls, 2010). The PDF and CLLF fault traces are drawn after rotation of the eastern block (solid lines) and again after additional restoration of N-S shortening as estimated in Fig. 6 (dotted lines). The Moho and Ps mantle discontinuity shown in the section were taken from Snyder et al. (2021). Geometrical patterns of Paleoproterozoic dyke swarms in the Superior craton and paleomagnetic**
420   **studies of those dykes both indicate relative motion across the Kapuskasing Structural Zone (KSZ) that divides the craton into eastern and western parts (Fig. 1) (Evans and Halls, 2010). Euler parameters that optimally group the paleomagnetic remanence data from six dyke swarms with ages between 2.47 and 2.07 Ga indicate a restoration of the eastern Superior relative to a 'pinned' western part about an Euler pole at 51°N, 85°W, with a rotation angle of 14° CCW (Fig. 13). Dyke strikes on either side of the KSZ align best after application of 23° CCW distributed shear composed of 90 km of sinistral transpressional displacement. Half of this**
425   **shear appears as distributed strain within the KSZ, half as oblique lateral thrusting (with NE-vergence) across the Ivanhoe Lake shear zone at ca. 1.90 Ga (Evans and Halls, 2010).**

4.2 Long-lived diverse history of some Superior faults

The southern Superior craton underwent a diverse history of deformation prior to its stabilization as a craton at about 2.65 Ga. Much of this strain history is recorded in its major fault zones, several of which will be highlighted here.

430   The Cadillac-Larder Lake fault (CLLF) forms a largely vertical east-west structure about 450 km long across the eastern half of the southern Superior craton (Fig. 1) (e.g., Bedeaux et al., 2017; Dubé & Mercier-Langevin, 2020). Several deep seismic reflection profiles that cross the fault zone indicate that it cuts the entire crust (Fig. 4). As discussed previously, the CLLF probably formed coeval with the upper crustal greenstones and TTG gneisses. Modern analogy with the Lau Basin of the western Pacific, specifically the Peggy's Ridge fault, suggests it formed a transform fault connecting triple junctions amid

435   several micro-oceanic plates (Baxter et al., 2020). Field studies suggest that segments of the fault were active during all known deformations affecting the Abitibi terrane (Bedeaux et al., 2017). Strong conductors at 60-90 km depths beneath the Kirkland Lake area and in several sub-vertical zones within the crust near this fault suggest that late migrating carbon- or sulfide-rich fluids left residuals (Wannamaker et al., 2014; Roots et al., 2022; 2024).

The Porcupine-Destor fault (PDF) parallels the Cadillac-Larder Lake fault zone about 200 km to its north (Fig. 1).

440   Within the central third of its mapped length, seismic reflection sections constrain its upper crustal attitude as dipping 25-35° to the south within the greenstone layer (Snyder et al., 2008; Haugaard et al., 2022). Near Timmins the dip may have been steepened by late differential horizontal shortening; in the mid-crustal (TTG) gneiss layer, conductors and attenuated reflectors suggest a steeper southward dip (Fig. 8) (Haugaard et al., 2022; Adetunji et al., in review). A Ps seismic discontinuity within the uppermost mantle near Kirkland Lake (Naghizadeh et al., 2022) may indicate the deeper

445   continuation of this lithospheric-scale fault, now offset 70 km southward relative to its mapped surface location (Fig. 10). Considered together, the DPF and CLLF could represent strain partitioning during peak D3 N-S shortening, with the DPF absorbing the N-S shortening and the CLLF accommodating oblique components of convergence (e.g., Haq and Davis, 2010).

The Sydney Lake fault in the western Superior craton (Fig. 1) was interpreted as nearly vertical within the upper half of the

450   crust and its base truncated at a gently south-dipping horizontal reflector (Calvert et al., 2004). It probably represents a fault that similarly partitioned N-S shortening and oblique strike-slip strains between the North Caribou and Winnipeg River terranes during their protracted convergence between 2.75 and 2.65 Ga (Hrabi and Cruden, 2006; Hynes and Song, 2006). A new interpretation of reprocessed seismic reflectors indicates a series of interleaved thrust wedges of greenstone crust (Fig. 11). Two hundred kilometers to the south, the Quetico fault probably played the same tectonic role between the Quetico and

455   Marmion/Wabigoon terrane boundary (Fig. 12) (Hendrickson, 2016). Restoring the multiple reversals of partitioned strike-slip along these upper crustal faults remains unresolved.

The Hawthorne Lake and Ivanho Lake faults comprise the main thrust faults bounding the Kapuskasing uplifted block and thus have major 2.07–1.87 Ga rotational displacements (Percival and West, 1994), but this Proterozoic strain may also mask earlier deformation, not yet recognized.

460 Conductivity models aid interpretation of seismic reflectors by 3D mapping of subsequent (late) fluid flow pathways. Crustal or even lithospheric-scale fault and shear zones appear to focus and concentrate large volumes of fluids that transport conductive minerals such as carbon and sulfides (Hill et al., 2021; Roots et al., 2022). In the Timmins area (Fig. 8), we interpret reduced reflection amplitudes to originate from pervasive metasomatism associated with these fluids reducing density and wave-speed contrasts at rock layer contacts. Enhanced conductivity resulted from residuals of carbon, metals,

465 and sulphides left behind by the same metasomatic fluids. These melts and fluids moved either by slow (millions of years), pervasive (bulk) vertical percolation (Gibson and McKenzie, 2023), by steep, channelized flow across nearly horizontal rock layers (Snyder et al., 2008; Heinson et al. 2018) or along contacts between moderately dipping rock layers, fractures or shear zones (Hill et al., 2021) as is more typically observed near Archean-Proterozoic boundaries (e.g., Aulbach et al., 2013). Similar flow mechanisms transport melts upward from the mantle into the crust where some erupt directly to the surface as

470 lamprophyres and kimberlites. Other fluids and melts stagnate in the mid-crust, possibly within magma reservoirs below the brittle-ductile transition (Hill et al., 2021). Flow to the surface then occurs either via high-strain zones characterized by near-vertical axial planes or in locations where intersecting major structures create low-strain regions where fluids can flow. The former structures are typical settings for small volume ore deposits whereas the latter host major deposits such as Olympic Dam, Timmins, and Malartic (e.g., Heinson et al., 2018; Dubé & Mercier-Langevin, 2020). Thus, specific structures and

475 tectonic history at all levels of the lithosphere influence which parts of Archean cratons become relatively well-endowed with metals (and diamonds) and which do not. A period of peak metamorphic conditions and prominent horizontal shortening within the upper crust of the Superior craton at 2.75-2.68 Ga coincides with mobilization of some metals (Au and rare metals) and resetting of mantle ages (Smit et al., 2014). This suggests a mineralization system was active at this time throughout the upper lithosphere.

5 Conclusions

The geometry of major inactive and ancient faults at depth must be mapped using high-resolution geophysical surveys such as reflection profiling, supported by conductivity models based on magnetotelluric current observations. Here a subset of deep reflection profiles recently acquired in the Archean southern Superior craton of North America provides such data with which to map some major shear zones, many of which host significant orogenic gold or VMS deposits. New (form) line

485 drawings of prominent reflectors grouped these reflectors as upper crustal or mid-crustal based on their intersections: upper crustal reflectors intersected (crocodiles) whereas mid-crustal ones appear mostly parallel (lamellae). Brittle, mafic-felsic lavas (greenstones) probably form the upper crust whereas ductilely deforming TTG gneisses form the middle crust.

Most faults are (re)interpreted as low-angle thrusts; a few notable exceptions appear as breaks in prominent reflectors aligned sub-vertically. Major near-vertical shear zones such as the Cadillac-Larder Lake fault probably originated co-eval

490 with eruption of the upper crustal greenstones, later reactivated as lithospheric-scale partitioned horizontal strain. Thrusting probably relates to the dominant phase of folding and horizontal shortening strain that occurred during the Kenoran (D_3)

crustal deformation, mineralization and peak metamorphism at 2.72-2.66 Ga. Most deformation after D$_3$ was associated with modest lateral displacements not recognized on the seismic sections.

Conductivity models of the 3-D crust around the seismic profiles indicate that some faults acted as conduits for late metasomatic fluid flow, while others did not. This channelized flow was probably a slow percolation process, crossing individual reflectors within near-vertical zones of thrust wedging. Proterozoic faults appear limited and local to the Kapuskasing uplift structure.

Author contribution

DS: Writing – original draft preparation. JS, TJ: Figures. All: Writing – review & editing. DS, JA: Conceptualization & Funding acquisition. MN, SC: seismic data processing. AA, GH, ER: magnetotelluricdata modelling & interpretation.

Acknowledgements

Seismic reflection and magnetotelluric data can be obtained from the Metal Earth Hub website (https://metalearth.geohub.laurentian.ca/search?tags=Dataset); see also Simmons et al., 2024 for more information. A GOCAD 3D model of the Superior mantle is available as a NRCan Open File report 8756. Metal Earth is funded by the Canada First Research Excellence Fund. Metal Earth contribution MERC-ME-2025-xx.

Competing Interests

The contact author has declared that none of the authors has any competing interests.

References

Abbott, D. H., Mooney, W. D., and VanTongeren, J. A.: The character of the Moho and lower crust within Archean cratons and the tectonic implications. Tectonophysics, 609, 690-705, 2013.

Adetunji, A. Q., Ferguson, I. J. Simmons, J. M., Chong Ma, Cheraghi, S., Snyder, D. B., and Ayer, J. A.: Trans-crustal geophysical responses beneath the supergiant Timmins-Porcupine orogenic gold camp, Canada. J. Geophys. Res. - Solid Earth, in review.

Artemieva, I. M. and Shulgin, A.: Making and altering the crust: A global perspective on crustal structure and evolution. Earth Planetary Sci. Letters, 512, 8-16, 2019.

Aulbach, S., Griffin, W. L., Pearson, N. J. and O'Reilly, S. Y.: Nature and timing of metasomatism in the stratified mantle lithosphere beneath the central Slave craton (Canada). Chem. Geol., 352, 153-169, 2013.

Ayer, J., Amelin, Y., Corfu, F., Kamo, S., Ketchum, J., Kwok, K., and Trowell, N.: Evolution of the southern Abitibi greenstone belt based on U-Pb geochronology: autochthonous volcanic construction followed by plutonism, regional deformation and sedimentation. Precam. Res., 115, 63–95, 2002.

Ayer, J. A., Berger, B. R., Hall, L. A. F., Houle, M. G., Johns, G. W., Josey, S., et al.: Geological compilation of the central Abitibi greenstone belt: Kapuskasing Structural Zone to the Quebec border, Map P.3565, scale 1:250 000, Sudbury, ON, Ontario Geological Survey, 2005.

Baxter, A. T., Hannington, M. D., Stewart, M. S., Emberley, J. M., Breker, K., Krätschell, A., Petersen, S., Brandl, P. A., Klischies, M., Mensing, R. and Anderson, M. O.: Shallow seismicity and the classification of structures in the Lau back-arc basin. Geochem. Geophys. Geosys., 21(7), p.e2020GC008924, 2020.

Beakhouse, G. P.: The Abitibi Subprovince plutonic record: Tectonic and metallogenic implications. Ontario Geological Survey, Open File Report 6268, 161p, 2020.

Bédard, J. H., and Harris, L.B.: Neoarchean disaggregation and reassembly of the Superior Craton. Geology, 42, 951–954, 2014.

Bedeaux, P., Pilote, P., Daigneault, R., and Rafini, S.: Synthesis of the structural evolution and associated gold mineralization of the Cadillac Fault, Abitibi, Canada. Ore Geol. Rev., 82, 49–69, 2017.

Bellefleur, G., Barnes, A., Calvert, A., Hubert, C. and Mareschal, M.: Seismic reflection constraints from Lithoprobe line 29 on the upper crustal structure of the northern Abitibi greenstone belt. Can. J. Earth Sci., 32(2), 128-134, 1995.

Benn, K.: Tectonic delamination of the lower crust during Late Archean collision of the Abitibi-Opatica and Pontiac terranes, Superior Province, Canada. In K. Benn, J.-C. Mareschal, K. Condie (Eds.), *Archean Geodynamics and Environments, Geophysical Monograph Series* (Vol. 164, 267–282,). Washington DC: American Geophysical Union, 2006.

Benn, K., and Peschler, A. P.: A detachment fold model for fault zones in the Late Archean Abitibi greenstone belt. Tectonophysics, 400, 85–104, 2005.

Bjorkman, K. E.: Crust-mantle evolution of the Western Superior Craton: implications for Archaean granite-greenstone petrogenesis and geodynamics (PhD thesis). University of Western Australia, Perth. doi: 10.4225/23/5a39c88a2f559, 2017.

Bleeker, W.: Synorogenic gold mineralization in granite-greenstone terranes: the deep connection between extension, major faults, synorogenic clastic basins, magmatism, thrust inversion, and long-term preservation. Geological Survey of Canada Open File 7852, 25–47, 2015.

Calvert, A. J., and Ludden, J. N.: Archean continental assembly in the southeastern Superior Province of Canada. Tectonics, 18, 412–429, 1999.

Calvert, A. J., Cruden, A. R., and Hynes, A.: Seismic evidence for preservation of the Archean Uchi granite–greenstone belt by crustal-scale extension. Tectonophysics, 388, 135–143, 2004.

Calvert, A. J., Sawyer, E. W., Davis, W. J., and Ludden, J. N.: Archean subduction inferred from seismic images of a mantle suture in the Superior Province. Nature, 375, 670–674, 1995.

Card, K. D.: A review of the Superior Province of the Canadian Shield, a product of Archean accretion. Precam. Res., 48, 99–156, 1990.

Cheraghi, S., Malehmir, A., Vayavur, R., Shamsipour, P., Naghizadeh, M., Haugaard, R., Snyder, D. B. and Ayer, J.: Addressing geometrical attributes and seismic imaging capability of fault systems in a world-class metal endowed region: Abitibi Greenstone Belt, Canada. Tectonophysics, 833, 229361, 2022.

Colpron, M., Nelson, J. L., and Murphy, D. C.: Northern Cordilleran terranes and their interactions through time. GSA Today, 17(4/5), 4, 2007.

Cook, F. A., White, D. J., Jones, A. G., Eaton, D. W., Hall, J. and Clowes, R. M.: How the crust meets the mantle: Lithoprobe perspectives on the Mohorovičić discontinuity and crust–mantle transition. Can. J. Earth Sci., 47, 315–351, 2010.

Daigneault, R., Mueller, W. U., and Chown, E. H.: Oblique Archean subduction: accretion and exhumation of an oceanic arc during dextral transpression, Southern Volcanic Zone, Abitibi Subprovince Canada. Precam. Res., 115, 261–290, 2002.

Daoudene, Y., Tremblay, A., Ruffet, G. and Leclerc, F.: The Abitibi-Opatica transition, Superior Province, Quebec, Canada: structural analysis, 40Ar/39Ar thermochronology and implications for Archean tectonics. Precam. Res., 379, 106803, 2022.

Davis, D. W., Sutcliffe, R. H. and Trowell, N. F.: Geochronological constraints on the tectonic evolution of a late Archaean greenstone belt, Wabigoon Subprovince, Northwest Ontario, Canada. Precam. Res., 39, 171–191, 1988.

Dimroth, E. and Rocheleau, M.: Archean wrench fault tectonics and structural evolution of the Blake River Group, Abitibi Belt, Quebec: Discussion. Can. J. Earth Sci., 22, 941–943, 1985.

Dubé, B., and Mercier-Langevin, P.: Gold deposits of the Archean Abitibi Greenstone Belt, Canada. In Geology of the World's Major Gold Deposits and Provinces, Special Publication, Soc. Econ. Geol., 23, https://doi.org/10.5382/SP.23.32, 2020.

Evans, D. A. D. and Halls, H. C.: Restoring Proterozoic deformation within the Superior craton. Precam. Res., 183, 474–489, 2010.

Fam, H. J. A., Naghizadeh, M., Smith, R., Yilmaz, O., Cheraghi, S., and Rubingh, K.: High-resolution 2.5 D multifocusing imaging of a crooked seismic profile in a crystalline rock environment: Results from the Larder Lake area, Ontario, Canada. *Geophysical Prospecting*, *71*(Special Issue: Mineral Exploration and Mining Geophysics), 1152-1180, 2023.

Frederiksen, A. W., Miong, S. K., Darbyshire, F. A., Eaton, D. W., Rondenay, S., and Sol, S.: Lithospheric variations across the Superior Province, Ontario, Canada: Evidence from tomography and shear wave splitting. J. Geophys. Res.: Solid Earth, 112(B7), B07318, doi:10.1029/2006JB004861, 2007.

Gibson, S. A. and McKenzie, D.: On the role of Earth's lithospheric mantle in global volatile cycles. Earth Planet. Sci. Lett., 602, 117946, 2023.

Goodwin, A. M. and Smith, I. E. M.: Chemical discontinuities in Archean metavolcanic terrains and the development of Archean crust. Precam. Res., 10, 301–311, 1980.

Grandjean, G., Wu, H., White, D., Mareschal, M., and Hubert, C.: Crustal velocity models for the Archean Abitibi greenstone belt from seismic refraction data. Can. J. Earth Sci., 32, 149–166, 1995.

585 Hacker, B. R., Kelemen, P. B. and Behn, M. D.: Continental lower crust. Ann. Rev. Earth Planet. Sci., 43, 167–205, 2015.

Haq, S. S. and Davis, D. M.: Mechanics of fore-arc slivers: Insights from simple analog models. Tectonics, 29(5), TC5015, doi:10.1029/2009TC002583, 2010.

Haugaard, R., Della-Justina, F., Roots, E., Cheraghi, S., Vayavur, R., Hill, G., Snyder D., Ayer, J., Naghizadeh, M., Hill, G., and Smith, R.: Crustal-scale geology and fault geometry along the gold endowed Matheson Transect of the Abitibi

590 Greenstone Belt. Econ. Geol., 116(5), 1053–1072. doi.org/10.5382/econgeo.4813, 2021.

Heinson, G., Didana, Y., Soeffky, P., Thiel, S., & Wise, T.: The crustal geophysical signature of a world class mineral system. Scientific reports, 8(1), 1–6, 2018.

Hendrickson, M. D.: Structural analysis of aeromagnetic data from the Rainy River Block, Wabigoon subprovince, Minnesota, USA and Ontario, Canada: Strain partitioning along a Neoarchean terrane boundary and implications for mineral

595 exploration. Precam. Res., 286, 20-34, 2016.

Herzberg, C.: Understanding the Paleoproterozoic Circum-Superior Large Igneous Province constrains the thermal properties of Earth's mantle through time. Precam. Res., 375, 106671, 2022.

Hill, G. J., Roots, E. A., Frieman, B. M., Haugaard, R., Craven, J. A., Smith, R. S., Snyder, D. B., Zhou, X., and Sherlock, R.: On Archean craton growth and stabilisation: insights from lithospheric resistivity structure of the Superior Province.

600 Earth Planet. Sci. Lett., 562, doi:10.1016/j.epsl.2021.116853, 2021.

Hrabi, R. B., and Cruden, A. R.: Structure of the Archean English River subprovince: implications for the tectonic evolution of the western Superior Province, Canada. Can. J. Earth Sci., 43, 947–966, 2006.

Hynes, A. and Song, Z.: Variable unroofing in the western Superior Province-metamorphic evidence and possible origin. Can. J. Earth Sci., 43, 805–819, 2006.

605 Langford, F. F., and Morin, J. A.: The development of the Superior Province of northwestern Ontario by merging island arcs. Am. J. Sci., 276, 1023–1034, 1976.

Leclerc, F., Harris, L. B., Bédard, J. H., van Breemen, O., and Goulet, N.: Structural and Stratigraphic Controls on Magmatic, Volcanogenic, and Shear Zone-Hosted Mineralization in the Chapais-Chibougamau Mining Camp, Northeastern Abitibi, Canada. Econ. Geol., 107, 963–989, 2012.

610 Lee, J., Tsai, V.C., Hirth, G. *et al.* Fault-network geometry influences earthquake frictional behaviour. *Nature* **631**, 106–110 (2024). https://doi.org/10.1038/s41586-024-07518-6

Ma, C., Naghizadeh, M., Adetunji, A. Q., Lodge, R.W.D., Snyder, D. B., and Sherlock, R.: Imaging Neoarchean crustal structures: An integrated geologic-seismic-magnetotelluric study in the western Wabigoon and Winnipeg River terranes, Superior craton. Precam. Res., 364, doi.org/10.1016/j.precamres.2021.106339**,** 2021.

615 Macpherson, C. G. and Hall, R.: Timing and tectonic controls in the evolving orogen of SE Asia and the western Pacific and some implications for ore generation. Geol. Soc. London, Spec. Pub., 204(1), 49–67, 2002.

Mathieu, L. and Leybourne, M.: Petrogenesis of a TTG intrusive suite: the La Dauversière pluton, Abitibi greenstone belt, Canada. Can. J. Earth Sci., in review.

Mathieu, L., Crépon, A. and Kontak, D. J.: Tonalite-dominated magmatism in the Abitibi subprovince, Canada, and
620 significance for Cu-Au magmatic-hydrothermal systems. Minerals, 10(3), 242, 2020.

Mathieu, L., Snyder, D. B., Bedeaux, P., Cheraghi, S., Lafrance, B., Thurston, P., and Sherlock, R.: Deep into the Chibougamau area, Abitibi greenstone belt: Structure of a Neoarchean crust revealed by seismic reflection profiling. Tectonics, 38, e2020TC006223. https://doi.org/10.1029/2020TC006223 2020.

McCaffrey, R.: The tectonic framework of the Sumatran subduction zone. Ann. Rev. Earth Planetary Sci., 37(1), 345–366,
625 2009.

Mints, M. V.: The composite North American Craton, Superior Province: Deep crustal structure and mantle-plume model of Neoarchaean evolution. Precam. Res., 302, 94–121, 2017.

Mole, D. R., Thurston, P. C., Marsh, J. H., Stern, R. A., Ayer, J. A., Martin, L. A. J., and Lu, Y. J.: The formation of Neoarchean continental crust in the south-east Superior Craton by two distinct geodynamic processes. Precam. Res., 356,
630 106104, 2021.

Monecke, T., Mercier-Langevin, P., and Dubé, B.: Archean Base and Precious Metal Deposits, Southern Abitibi Greenstone Belt, Canada, in: Reviews in Economic Geology, v. 19, Society of Economic Geologists. doi:10.5382/Rev.19, 2017.

Mooney, W. D.: 1.11 crust and lithospheric structure–global crustal structure. Seismology and Structure of the Earth: Treatise on Geophysics, 1, 361, 2010.

635 Mueller, W. and Donaldson, J. A.: Development of sedimentary basins in the Archean Abitibi belt, Canada: an overview. Can. J. Earth Sci., 29, 2249–2265, 1992.

Musacchio, G., White, D. J., Asudeh, I., and Thomson, C. J.: Lithospheric structure and composition of the Archean western Superior Province from seismic refraction wide angle reflection and gravity modeling. J. Geophys. Res.: Solid Earth, 109, B03304, doi:10.1029/2003JB002427, 2004.

640 Naghizadeh, M., Smith, R., Rubingh, K., Sherlock, R., Ayer, J., Lafrance, B., Cheraghi, S., Snyder, D., Vergne, J., Hollis, D. and Mordret, A.: Active and passive seismic imaging of the central Abitibi greenstone belt, Larder Lake, Ontario. J. Geophys. Res.: Solid Earth, 127(2), p.e2021JB022334, 2022.

Naghizadeh, M., Snyder, D., Cheraghi, S., Foster, S., Cilensek, S., Floreani, E., and Mackie, J.: Acquisition and Processing of Wider Bandwidth Seismic Data in Crystalline Crust: Progress with the Metal Earth Project. Minerals, 9(3), 145, 2019.

645 Okaya, D. A. and Jarchow, C. M.: Extraction of deep crustal reflections from shallow Vibroseis data using extended correlation. Geophysics, 54, 555–562, 1989.

Percival, J. A., and West, G. F.: The Kapuskasing uplift: A geological and geophysical synthesis. Can. J. Earth Sci., 31, 1256–1286, 1994.

Percival, J. A., Sanborn-Barrie, M., Skulski, T., Stott, G. M., Helmstaedt, H., and White, D. J.: Tectonic evolution of the
650 western Superior Province from NATMAP and Lithoprobe studies Can. J. Earth Sci., 43, 1085–1117, 2006.

Percival, J. A., Skulski, T., Sanborn-Barrie, M., Stott, G. M., Leclair, A. D., Corkery, M. T., and Boily, M.: Geology and tectonic evolution of the Superior Province, Canada. Chapter 6, in: Percival, J.A., Cook, F.A. Clowes, R.M. (eds.). Tectonic

Styles in Canada: The LITHOPROBE Perspective. J. A. Percival, F.A., Cook, R. M Clowes, (eds.). Geol. Assoc. Canada, Special Paper 49, 321–378, 2012.

655 Poulsen, K. H.: The Larder Lake-Cadillac Break and its gold districts, Rev. Econ. Geol., 19, 133–167, 2017.

Roots, E. A., Frieman, B. M., Hill, G. J., Smith, R. S., Craven, J. A., Calvert, A. J. and Snyder, D. B.: Constraints on growth and stabilization of the western Superior Craton from inversion of magnetotelluric data. Tectonics, 43(5), p.e2023TC008110, 2024.

Roots, E. A., Hill, G. J., Frieman, B. M., Wannamaker, P. E., Maris, V., Calvert, A. J., Craven, J. A., Smith, R. S. and
660 Snyder, D. B.: Magmatic, hydrothermal and ore element transfer processes of the southeastern Archean Superior Province implied from electrical resistivity structure. Gondwana Res., 105, 84–95, 2022.

Rudnick, R. L. and Fountain, D. M.: Nature and composition of the continental crust: a lower crustal perspective. Rev. Geophys., 33(3), 267–309, 1995.

Sanborn-Barrie, M., and Skulski, T.: Sedimentary and structural evidence for 2.7 Ga continental arc–oceanic-arc collision in
665 the Savant–Sturgeon greenstone belt, western Superior Province, Canada. Can. J. Earth Sci., 43, 995–1030, 2006.

Schaeffer, A. J., and Lebedev, S.: Imaging the North American continent using waveform inversion of global and USArray data. Earth Planet. Sci. Lett., 402, 26–41, doi.org/10.1016/j.epsl.2014.05.014, 2014.

Simmons, J. M., Snyder, D. B., Ayer, J. A., Naghizadeh, M., Adetunji, A. Q., Jørgensen, T. R. C., Hill, G. J., Roots, E. A., and Saeid Cheraghi, S.: A Metal Earth Atlas of Seismic Reflection and Magnetotelluric Transects Across the Superior
670 Province. Laurentian University. doi: 10.1139/9780886671341, 2024.

Smit, K. V., Stachel, T., Creaser, R. A., Ickert, R. B., DuFrane, S. A., Stern, R. A., and Seller, M.: Origin of eclogite and pyroxenite xenoliths from the Victor kimberlite, Canada, and implications for Superior craton formation. Geochim. Cosmochim. Acta, 125, 308–337, 2014.

Snyder, D. B. and Thurston, P. C.: A North Caribou superterrane in the Superior craton, North America. Precam. Res., 403,
675 107329, 2024.

Snyder, D. B., Bleeker, W., Reed, L. E., Ayer, J. A., Houlé, M. G., and Bateman, R.: Tectonic and metallogenic implications of regional seismic profiles in the Timmins mining camp. Econ. Geol., 103, 1135–1150, 2008.

Snyder, D. B., Savard, G., Kjarsgaard, B. A., Vaillancourt, A., Thurston, P. C., Ayer, J. A., and Roots, E.: Multidisciplinary modelling of mantle lithosphere structure within the Superior Craton, North America. Geochem. Geophys. Geosys, doi
680 10.1029/2020GC009566, 2021.

Stern, T. A. and McBride, J. H.: Seismic exploration of continental strike-slip zones. Tectonophysics, 286, 63–78, 1998.

Szwillus, W., Afonso, J.C., Ebbing, J. and Mooney, W. D.: Global crustal thickness and velocity structure from geostatistical analysis of seismic data. J. Geophys. Res.: Solid Earth, 124, 1626–1652, 2019.

Thurston, P. C.: Autochthonous development of Superior Province greenstone belts?. Precam. Res., 115, 11–36, 2002.

685 Tikoff, B. and Teyssier, C.: Strain modeling of displacement-field partitioning in transpressional orogens. J. Structural Geol., 16, 1575–1588, 1994.

Tóth, Z., Lafrance, B. and Dubé, B.: Oblique lateral extrusion during dextral transpression along the Beardmore-Geraldton belt, Canada. J. Structural Geol., 169, 104834, 2023.

van der Velden, A. J. and Cook, F. A.: Relict subduction zones in Canada. J. Geophys. Res.: Solid Earth, 110(B8), 2005.

Wannamaker, P. E., Evans, R. L., Bedrosian, P. A., Unsworth, M. J., Maris, V., and McGary, R. S.: Segmentation of plate coupling, fate of subduction fluids, and modes of arc magmatism in Cascadia, inferred from magnetotelluric resistivity. Geochem. Geophys. Geosys., 15(11), 4230–4253, 2014.

White, D. J. , Musacchio, G., Helmstaedt, H. H., Harrap, R. M., Thurston P., van der Velden, A., and Hall, K.: Images of a lower-crustal oceanic slab; direct evidence for tectonic accretion in the Archean western Superior Province. Geology 31, 997–1000, 2003.

Žák, J., Svojtka, M., Sláma, J., Tomek, F., Kachlík, V., Ackerman, L., Vacek, F. and Trubač, J.: Exploring the link between spatiotemporal patterns of plutonism and geodynamic regimes at the end of Archean: an example from the northeastern Superior Province, Canada. Precam. Res., 392, 107073, 2023.

Žák, J., Tomek, F., Svojtka, M., Vacek, F., Kachlík, V., Ackerman, L., Ježek, J. and Petronis, M.S.: Distributed crustal shortening followed by transpressional shearing in the Superior Province, northeastern Canada: A Late Archean analogy to modern accretionary plate margins? Precam. Res., 362, 106322, 2021.

Zhang, J., Linnen, R., Lin, S., Davis, D., and Martin, R.: Paleoproterozoic hydrothermal reactivation in a Neoarchean orogenic lode gold deposit of the southern Abitibi Subprovince; U-Pb monazite geochronological evidence from the Young-Davidson Mine, Ontario. Precam. Res., 249, 263–272, 2014.